ANL-5717
Metallurgy and Ceramics

ARGONNE NATIONAL LABORATORY
P. O. Box 299
Lemont, Illinois

QUARTERLY REPORT
JANUARY, FEBRUARY, AND MARCH 1957

METALLURGY DIVISION

Frank G. Foote, Director
James F. Schumar, Associate Director
Haim H. Chiswik, Associate Director

March 31, 1957

Previous Quarterly Reports:

ANL-5709 October, November, December 1956
ANL-5643 July, August, September 1956
ANL-5623 April, May, June 1956

Operated by The University of Chicago
under
Contract W-31-109-eng-38

DISCLAIMER

TABLE OF CONTENTS

TABLE OF CONTENTS

METALLURGY DIVISION REPORTS AND PAPERS PUBLISHED DURING THE QUARTERLY PERIOD JANUARY - MARCH 1957

R. A. Bach, O. E. Layton and J. H. Handwerk, "Development and Operation of an Automatic Press for Ceramic Powders," ANL-5669 (January 1957).

W. J. McGonnagle, G. L. Kehl and Hyman Steinmetz, "The Removal of Inclusions for Analysis by an Ultrasonic 'Jack Hammer'," Metallurgia 55 151-154 (March 1957).

W. N. Beck, "An Ultrasonic Scanner and Recording System," Nondestructive Testing 15 (1) 42-43 (January-February 1957).

R. D. Misch, "Dissolution of the Oxide Film on Zirconium," Acta Metallurgica 5 179-180 (March 1957). Letter

A. H. Roebuck, C. R. Breden and Sherman Greenberg, "Corrosion of Structural Materials in High Purity Water," Corrosion 13 87-90 (January 1957).

David Meneghetti and S. S. Sidhu, "Magnetic Structures in Copper-Manganese Alloys," Phys. Rev. 105 130-135 (January 1, 1957).

Leroy Heaton and S. S. Sidhu, "Thermal-Neutron Coherent Scattering Amplitudes of Thallium and Osmium," Phys. Rev. 105 216-218 (January 1, 1957).

J. H. Handwerk and R. A. Noland, "Oxide Fuel Elements for High Temperatures," Chem. Eng. Prog. 53 60F-62F (February 1957).

J. H. Handwerk, L. L. Abernethy and R. A. Bach, "Thoria and Urania Bodies," Bull. Am. Cer. Soc. 36 99-101 (March 1957).

Bernhard Blumenthal and R. A. Noland, "High Purity Uranium" Progress in Nuclear Energy, Series V, Metallurgy and Fuels (London: Pergamon Press, Ltd., 1956) pp. 62-80.

F. G. Foote, "Physical Metallurgy of Uranium," Progress in Nuclear Energy, Series V, Metallurgy and Fuels (London: Pergamon Press Ltd., 1956) pp. 81-201.

K. F. Smith, "Radiations from the Atomic Industrial Forum," Metal Prog. 70 110-112 (November 1956).

QUARTERLY REPORT
JANUARY, FEBRUARY, AND MARCH 1957
METALLURGY DIVISION

ABSTRACT

Advanced Water Reactor Program - Activity 4102

The second core for EBWR is planned to consist of thoria-urania pellets enclosed in tube sheets, similar to the Borax-IV loading which is now under test. Higher temperature and strength requirements for the EBWR, however, make necessary the substitution of tube sheet material different than the aluminum alloy used for Borax-IV. Zircaloy-2 is a possible choice for tube sheet material, but extrusion of this material, unlike the aluminum, would be expected to be very difficult.

Alternate methods, including rolling and expansion, are being tried. These take the form of bonding two Zircaloy-2 plates together by rolling, but leaving lengthwise strips of unbonded areas which later can be expanded into tubes pneumatically. Efforts to date have been unsuccessful in establishing proper conditions for the intermittent bonding.

As for the fuel pellets themselves, experiments are under way to improve their thermal shock resistance by incorporating metal fibers into the sintered ceramic bodies. The use of reinforcing wire of molybdenum and of niobium is being studied as to possibility of reactions with the ceramic base and with several canning materials.

Studies are also being made on methods of producing sound pellets of thoria-urania with urania in excess of 30% by weight. Present techniques for these high urania compacts result in cracking and excessive porosity.

The use of fused thoria and urania in the preparation of high-density compacts is also receiving some preliminary attention.

Fast Power Breeder Program - Activity 4104

Techniques for casting billet cores for EBR-I, Core III are being developed. One method, a multiple type, has been successfully used for casting 8 billets of normal uranium simultaneously and is presently being extended to 16 for a potential production rate of 32 billets per day. The other method is for enriched cores and has been less successful. This is a single billet method and some difficulty has been encountered in magnesium deposits being formed in the mold. Magnesia crucibles are being used.

Work is also being done on joining methods required to permit fuel and blanket rod fabrication of EBR-I, Core III. These rods are to be made separately by coextrusion, cut into slugs, assembled in correct order, and butt-welded together. Following this, the assembly is to be heat treated, straightened and centerless ground The tip and spacing ribs will then be attached, the former being final machined in place for accurate centering.

From five prospective bidders on the construction and installation of equipment for the Fuel Fabrication Facility (Building 350), only one bid was returned and that one was excessive. The work has now been subdivided into seven categories for resubmission for bidding, with coordination responsibility remaining with Argonne.

Investigation of methods for the remote refabrication of irradiated alpha-active reactor fuels has been undertaken with primary direction of effort to EBR-II fuels. The basic tenet is that the process be accomplished by a minimum number of operations. Under limitations of the inert atmosphere necessary, and the use of hard, brittle fuel materials, precision casting has suggested the best possibilities, notwithstanding the long, narrow shape of the reference element core. An injection casting technique has been developed toward this end which has resulted in a satisfactory yield, even of the difficult casting uranium-fissium compositions. Other elements of the operation are now being modified for remote control.

The solidus temperature of U-10 w/o Fs has been measured as approximately 1000°C and of U-20 w/o Pu-10 w/o Fs as about 930°C.

Argonne Low Power Reactor - Activity 4202

A small number of ALPR fuel plates, made under development contracts, were sent to ANL for evaluation. These are made of aluminum-uranium alloy clad with aluminum alloy M-388. Boron to 0.5 w/o is present in the core alloy. Pertinent properties are being determined at the present time.

Advanced Engineering and Development - Activity 4530/4540

Disassembly of the damaged EBR-I, Core II has been completed and evaluation made. Details of the structure, with photographs, are included. Examination of the microstructure gives confirmation of alloying of the core with the stainless steel jacketing, with subsequent eutectic melting.

Development of fuel elements for the TREAT reactor has been initiated. This is proposed as a UO_2 dispersion in graphite. The use of graphite bonded with Bakelite or furfural alcohol appears to be feasible at this stage.

In nondestructive testing, billets for the EBR-I, Core III have been tested by ultrasonic methods, and an ultrasonic fluoroscopy unit is under construction, featuring barium titanate transducers. Further studies of eddy-current techniques are being made with the new dual channel system which cancels out the variable of probe-to-metal spacing. A considerable increase in sensitivity to defects is reported as a result of this innovation.

A new dynamic corrosion testing facility has been constructed which features more accurate control of dissolved constituents and replaceability of samples during operation of the system.

The development of an electrolytic cell to measure the pH of phosphoric acid solutions has resulted in a method of separating the corrosion effects of pH and anions in the testing of aluminum alloys. Attempts are being made to assess the effects of using phosphoric acid as a corrosion inhibitor in the EBWR.

Some preliminary corrosion results on magnesium alloys show superior resistance to those of high-purity magnesium. This is of interest because of their proposed use in "Mighty Mouse."

Certain zirconium capsules which failed in MTR irradiation have been examined in the metallographic cave to determine the cause of failure. The examination disclosed no effects traceable to radiation damage beyond the fact that the zirconium was Grade III, which is unsuitable for reactor applications.

Production, Treatment, and Properties of Materials - Activity 5410

Three fundamental elastic constants have been determined on the three single crystals of alpha uranium, as described in ANL-5709. The crystals were produced at ANL and measured at the Bell Telephone Laboratories by an ultrasonic method. Each crystal was cut parallel to one set of orthogonal planes, yielding at least one value of each of the normal constants C_{11} to C_{66}. Three more crystals of somewhat different orientations, which are designed to furnish the shear constants C_{12} to C_{56}, are in preparation. These will be sufficient to fully describe the elastic properties of single crystals of uranium.

Further metallographic work has been done on the recrystallization properties of alpha uranium, with further indication of a different mechanism operating below 380°C from that operating above that temperature. At present the thermal expansion coefficients are being compared for specimens annealed at low temperatures for long times and others annealed at high temperatures for short times.

The program to measure self-diffusion in uranium by sputtering a layer of U^{235} on depleted uranium has run into a snag owing to difficulties encountered in the formation of an unidentified "barrier layer" (ANL-5709). Efforts to eliminate this barrier, which included cleaning of the cathode by ionic bombardment, have so far been unsuccessful.

A thermal analysis apparatus has been constructed and determination made of the uranium-carbon eutectic temperature, which is shown to be 1116.5 ± 1.1°C. The melting point of high-purity uranium has also been redetermined at 1132.4 ± 0.6°C, mean of melting and freezing, which is in substantial agreement with previously measured values, both at the Bureau of Standards and at ANL.

The binary uranium-ruthenium system has been examined from 20 to 50 w/o Ru, showing six intermetallic compounds. The binary uranium-molybdenum system is being investigated as to the effect of molybdenum on the lattice parameter of the gamma phase. A preliminary version of the uranium-rich corner of the uranium-ruthenium-molybdenum ternary system has been developed.

Long-term corrosion tests (up to 1000 days) of 1100 aluminum in distilled water and potassium sulfate solutions are nearly complete and show, tentatively, a continuously decreasing rate. Improvement in the technique of measuring film resistance on zirconium alloys has resulted from the use of an electrometer in conjunction with a means of current measurement in series with the film drop. Two zirconium ternary alloys have survived 47 days in 400°C steam as follows: (1) 0.32 w/o Y, 0.68 w/o Nb, and (2) 0.03 w/o Sc, 0.47 w/o Th.

Sintering studies have been made on Al_2O_3 (sapphire spheres) in vacuum, helium and electrolytic hydrogen. On 30-mil spheres at 1800°C in hydrogen the mechanism appears to be volume diffusion modified by surface diffusion. At higher temperatures or with smaller spheres the mechanism seems to be solely volume diffusion. No sintering occurred in vacuum or helium.

Alloy Theory and the Nature of Solids - Activity 5420

The study of the role of atomic size in determining the occurrence and lattice parameter of Cr_3O-type phases has been completed and a paper has been submitted for open literature publication. A criterion for the stability of the phase in terms of a ratio of the radii of component atoms has been established, and empirical equations have been derived for predicting the lattice parameter of the phase from a knowledge of the atomic radii. The existence and composition ranges of sigma phases in Os-W, Os-Ta, and Ir-Ta have been established.

I. ADVANCED WATER REACTOR PROGRAM - ACTIVITY 4102

1. Development of Ceramic Fuel Elements

a. Fabrication of Zircaloy-2 Cladding for Ceramic Fuel Elements (J. R. Lindgren, C. H. Bean, R. E. Macherey)

The second fuel loading for the EBWR is planned as thoria-urania. This fuel is expected to be similar to that used in the Borax-IV loading, i.e., pellets jacketed in aluminum tube-in-sheet mechanically bonded with lead. Because of the higher service requirements, however, a substitution of Zircaloy-2 for the aluminum cladding becomes a possibility.

As an initial design specification of the cladding for the second loading of EBWR, the Borax-IV tube-in-sheet is being used. An end view of the aluminum cladding used for the Borax-IV loading is shown in Figure 1. This tube-in-sheet was produced by extrusion.

Figure 1. End View of Cladding Tube-in-Sheet for Borax IV.

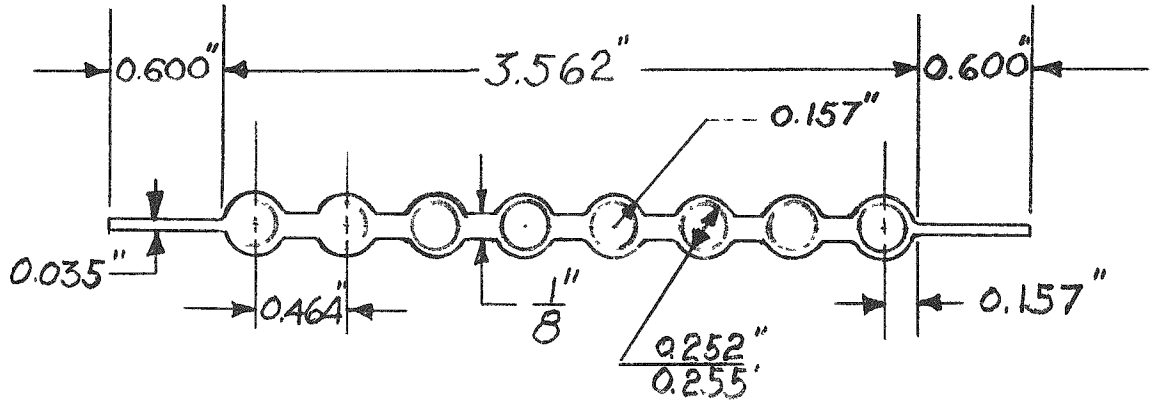

Extrusion of a similar tube-in-sheet of Zircaloy-2, however, would be extremely difficult. Two avenues of approach more practical than extrusion for the production of this type of cladding present themselves. These are forming and welding, and rolling and expansion. No work has been done on forming and welding; some work has been done on rolling and expansion.

The work which has been done was generally patterned after the process developed commercially for the production of copper and aluminum tube-in-sheet.

Two methods have been explored for making slotted sheet which then can be expanded into cladding jackets. The first tried was roll bonding. Shallow slots the width of one-half the circumference of the desired tube were machined in two Zircaloy-2 plates at proper locations of the desired tubes. The sheets were then placed, slotted sides together, with graphite strips placed within the slots. The sheets were pressed together and sealed by welding, and the assembly was jacketed in steel. The jacketed billet was then hot rolled at 850°C in an attempt to bond the plate in the webs between the slots and retain unbonding in the tube slots. Even with heavy reductions (90%) the plates were only partially bonded.

Because of the bonding difficulties and the need for extensive inspection of this type of product, a second method was tried. In this method, holes either square or round were drilled longitudinally at the center line of a plate and the holes filled with graphite rods to prevent bonding. After jacketing in steel the billets were rolled at 850°C into 50-mil sheet. No bonding developed in the tube slots.

First attempts to expand the slots into tubes were done pneumatically at room temperature. For introduction of the gas into the slots a Zircaloy-2 header was welded to one end of the sheet and the other end was sealed by welding. Because of the relatively low ductility of Zircaloy-2, the slots ruptured before much expansion took place.

Next attempts at expansion were done at elevated temperatures to improve the ductility of the material. Several different temperatures between 650° and 950°C were tried, but expansion of the slots into tubes was best done at 900°C. To reduce contamination of the strip at these elevated temperatures, the work was done in an argon atmosphere and expansion was also performed with argon. The outside diameter of the tubes varied from 0.245 to 0.277", averaging 0.260".

During the expansion of the tubes some warping developed in the sheet. Attempts to restrain the sheet by clamping between steel dies was unsuccessful because of the difference in thermal expansion coefficients of the die and work.

b. Metal Fibers in Thoria-Urania Ceramic Fuel Bodies
(C. L. Hoenig, R. C. Lied)

A series of thoria-urania fuel bodies reinforced with metal fibers of the type developed by Armour Research Foundation was fabricated for irradiation tests. These bodies have shown good resistance to thermal shock and to thermal fragmentation in out-of-pile tests.

Several sets of specimens were fabricated by hot pressing. One series of compositions was reinforced with molybdenum wire at 10 w/o, while a second series was reinforced with niobium wire at 10 w/o.

Specimens were made using both normal and enriched uranium, with urania-thoria ratios of 90/10, 70/30, and 50/50. These specimens measured approximately 3/8" in diameter and 1/2" in length. The apparent porosity of the specimens ranged from 2 to 17% for the specimens containing enriched urania, and from 2 to 25% for the specimens containing the normal urania.

Cans of Zircaloy-2 and Al-1% Ni have been made and the pellets are now in the process of being canned.

Possibility of reaction was studied at 600°, 700°, and 800°C between the following materials: UO_2-ThO_2 and Zircaloy-2; UO_2-ThO_2 and stainless steel; UO_2-ThO_2 and lead; lead and Zircaloy-2; lead and stainless steel; graphite and Zircaloy-2; graphite and UO_2-ThO_2.

In the first attempt couples of the samples were vacuum sealed in Vycor tubes and the tubes put in lead baths at the three operating temperatures. Lead oxide forming at the surface of the baths reacted with the Vycor tubing so rapidly that the method had to be abandoned.

For the second attempt the vacuum-sealed Vycor capsules were put in stainless steel tubes with fine silica as a shock shield between the samples. The heating medium used was a salt bath (Houghton's Liquid Heat 80). After 240 hours the stainless steel sample tubes were corroded through just below the surface of the salt. The salt bath was abandoned as a heating medium.

2. Properties of Thoria-Urania Bodies (C. L. Hoenig)

Thoria-urania bodies containing up to 30 w/o UO_2 have been successfully fabricated in small shapes by air-firing mixtures of ThO_2 and U_3O_8. Compositions containing more than 30 w/o UO_2 tend to crack when air-fired. These compositions also have low densities.

In an effort to improve the densities of thoria-urania bodies containing more than 30 w/o UO_2, -325 mesh ThO_2 and UO_2 were mixed in the ratio of 70 w/o ThO_2-30 w/o UO_2 and 50 w/o ThO_2-50 w/o UO_2. These powder mixes were then calcined in air at 600°C. Specimens measuring 1/4" and 3/4" in diameter were pressed from the calcined powders and fired to 1450° - 1500°C in 24 hours. The 1/4" pellets were found to be free of cracks while the 3/4" pellets were found to be cracked. X-ray analysis of the powder calcined at 600°C showed the orthorhombic structure similar to the U_3O_8 and faint ThO_2 lines. It is evident that the ThO_2-UO_2 solid solution is not found by calcining mixtures of thoria and urania powders at 600°C. The temperature at which these solid solutions form, and the nature of

their formation would appear to furnish the logical answer to fabrication of air-fired ThO_2-UO_2 solid solutions containing more than 30 w/o UO_2, and experiments designed to establish the temperature of formation are now in progress.

The use of fused UO_2 and ThO_2 in the preparation of high density thoria and urania bodies is also being investigated. An arc furnace has been set up and an attempt made to fuse ThO_2. Initial runs have produced a small amount of what appears to be ThO_2 glass.

II. FAST POWER BREEDER REACTOR PROGRAM - ACTIVITY 4104

1. EBR-I, Mark III Core Loading

a. Casting Extrusion Billet Cores (N. J. Carson, Jr., R. E. Macherey)

During the first quarter of 1957, foundry effort was confined to service work and to development of a casting technique for EBR-I, Mark III extrusion billet cores. Two separate techniques were pursued: one for casting several normal uranium alloy cores simultaneously, and the other for individual enriched uranium alloy cores..

The normal uranium alloy cores have been successfully cast using a one-piece graphite mold consisting of eight cylindrical cavities arranged radially in a 10" diameter, 12" long, graphite cylinder. A pouring cup was cut into the top center of the mold and connected by spillways to the individual cavities. Using a pouring temperature of 1400°C, sound and homogeneous castings can be consistently produced. Effort is now being extended to the production of 16 cores from a single heat. When this is achieved the potential production rate will be 32 cores per day.

The method of casting enriched cores involves the use of magnesia crucibles, split type, single cavity graphite molds, and zirconium wire. The most desirable castings have been made using pouring temperatures between 1385° and 1400°C. The most suitable mold temperature has not yet been established.

A great deal of difficulty has been experienced with magnesium deposits forming in the mold. There is evidence that the crucibles now being used are decomposing at lower temperatures than did those of previous batches. Figure 2 shows magnesium deposited on the side of a mold into which a uranium alloy had been poured. Figure 3 shows the magnesium deposit taken from a mold bottom following a heat which could not be poured. In both instances the diagnosis of magnesium was confirmed by X-ray diffraction.

At the present time magnesium deposition in the mold is prevented by a 1/2" vent space between mold and crucible assembly and by a perforated uranium foil disc in the mouth of the mold. The foil disc prevents magnesium from entering the mold, but offers very little resistance to the passage of superheated uranium.

The billet core castings after machining will be jacketed with Zircaloy-2, canned in copper, and extruded into rod at Nuclear Metals, Inc. The finished rods will be 0.404" outside diameter, clad with 0.020" of Zircaloy-2. The ribs required for spacing rods for the rigid core loading will be welded-on wires.

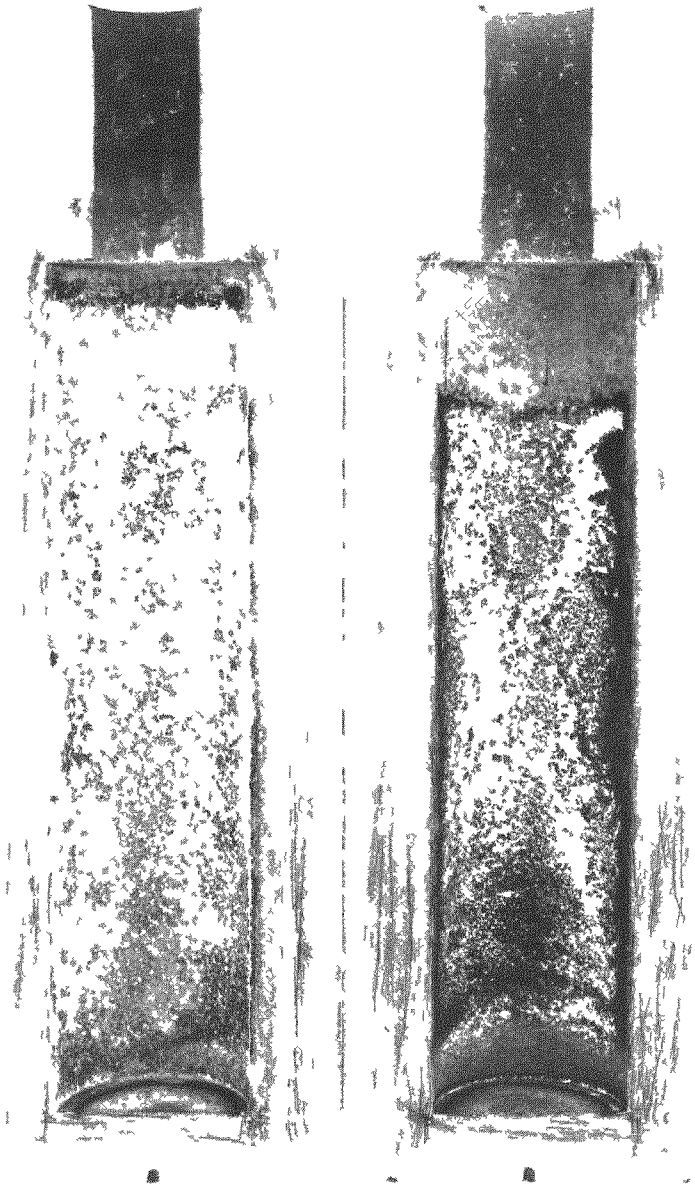

Macro 21154 5/8-X

Figure 2

Magnesium Deposit Found on Mold Wall Following Removal of Casting.

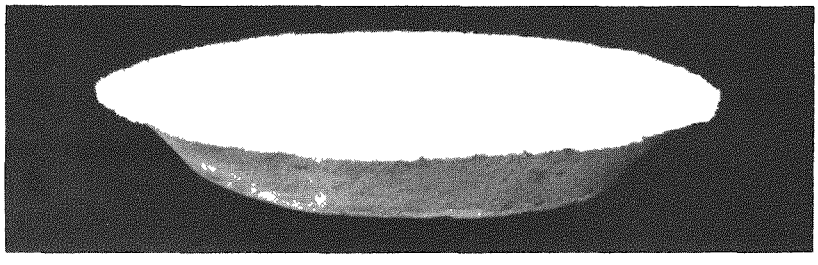

Macro 21373 2-X

Figure 3

Magnesium Deposit Taken from Bottom of Mold (Heat Not Poured).

b. Welding of Fuel and Blanket Rods (R. A Noland, C. C Stone, F. D. McCuaig)

Work has continued during the past quarter on the development of joining methods required to permit fabrication of the fuel rods and blanket rods for the Mark III core of EBR-I With the exception of an 8.500" long central section of each fuel rod in which the uranium present is 93 5% U^{235}, both rod types are identical. The rods are 0.403 ± 0 001" diameter by 21¾" long (without handle) and are clad with a 0 020" layer of Zircaloy-2 by coextrusion. A U-2 w/o Zr alloy provides the core material; in the blanket rods the uranium is present as natural uranium, blanket sections of the same composition and enrichment are fastened to each end of the heavily enriched fuel section in the fuel rods. Thin Zircaloy-2 discs are used to separate the fuel sections from the blanket sections. All rods have an accurately machined Zircaloy-2 locating tip at one end. A Zircaloy-2 fitting, which is drilled and tapped to receive a stainless steel handle, is fixed to the opposite end. To space the rods in the reactor core, three longitudinal fins, 0.043 to 0.047" high, are spaced 120° apart around the periphery of each rod.

Fabrication: Clad lengths of rod of the blanket composition and the fuel composition are to be produced by coextruding billets of the desired material canned in Zircaloy-2. The extruded lengths will be cut into slugs; the enriched extrusions into 8.500" long sections, the natural enrichment extrusions into fuel rod blanket slugs 3.562" and 7.750" long, and into blanket rod sections 19.812" in length. To form either type rod, the appropriate sections will be assembled, accurately positioned, and then butt-welded together The butt-welded rods will next be heat treated, straightened, and sized by removing 0.005" or less from their outer diameters in a centerless grinding operation. The locating tip mounted on one end of each rod will then be machined in place so as to put its center line precisely coincident with the longitudinal center line of the rod. Following this, the longitudinal spacing ribs will be welded in place. It has not as yet been decided whether it will be necessary to size the ribs after welding.

As indicated earlier, work has continued during the past quarter on the development of suitable welding techniques for (1) butt-welding, and (2) attachment of the spacing rubs.

Butt-Welding. It is desired that the butt-welding include a seal weld at the clad-to-clad junction and that most of the area of the abutting surfaces be joined. Dimensional alignment of the sections after welding is rigidly limited; coincidence (run out) of the center lines of the joined sections must be held to within 0.002". Two basic approaches have been investigated, namely, (1) electric resistance welding, and (2) a combination of inert gas, tungsten-arc and induction welding. Results obtained in

a small number of exploratory trials of the electric resistance butt-welding approach were discouraging, so the work on this technique was discontinued. Rather encouraging welds have been produced by a method in which inert-gas, tungsten-arc welding achieves the clad-to-clad seal weld, which is followed by induction welding to fuse the abutting surfaces of the adjoining sections. Apparatus to perform both welding operations on a semiautomatic, more reproducible basis is now being constructed

Spacing Rib Welding: Satisfactory attachment of the Zircaloy-2 spacer ribs has been shown to be feasible by electric resistance spot welding on a condenser-discharge type unit. Passage of the work through the welding operation was done by hand in the work to date A fully automated device which will automatically feed the work through the machine is now being built. This device is expected to be used in the production run.

2. EBR-II Fuel Fabrication (A. B. Shuck, F. L. Yaggee, J. E. Ayer, R. M. Mayfield, H. F. Jelinek)

a. Equipment for the Fuel Fabrication Facility (Facility #350)

The designing of the equipment for Facility #350 was completed during the quarter. Mechanical construction bids were solicited from five contractors who in previous contacts had indicated a willingness to attempt to lump-sum bid the work. "No bid" was returned by the O. G. Kelley Company, by the Pittsburgh Piping and Equipment Company, by Swinerton and Walberg Company, and by the Consolidated Western Steel Division of the U.S. Steel Company. A bid was opened on February 28 from the Blaw-Knox Company for the amount of $5,285,000. This bid greatly exceeded the total amount available for the work and estimates by both ANL engineers and the architect-engineers; the bid was rejected.

Investigation of the "no bid" returns indicated that failure to bid was due in part to the reluctance of general contractors to bid on work of an unfamiliar nature and to the reluctance of manufacturing contractors to undertake an involved installation contract.

It was therefore determined to break the work down into seven parts of known familiarity to subcontractors and for the Laboratory to assume the responsibility for the coordination and administration of these subcontracts. The specification is therefore being rewritten in the following parts:

Part II-A Fabrication of Hoods, Subhoods, Enclosures and Miscellaneous Equipment

Part II-B Installation of Hoods, Subhoods, Enclosures and Process Equipment

Part II-C Process Piping

Part II-D Ventilation and Sheet Metal Work

Part II-E Electrical Work

Part II-F Pneumatic Controls

Part II-G Painting

Bids will be solicited on each of the above parts with the contractors encouraged to bid on more than one part.

b. Development of Methods for the Remote Refabrication of Irradiated ($\alpha + \gamma$ Radioactive) Reactor Fuels

The investigation of methods for the remote refabrication of irradiated reactor fuels has been undertaken with the objective of designing, constructing, and testing techniques and equipment for the refabrication of EBR-II fuels. Studies have been made to establish the basic requirements for remote controlled refabrication processes. Preliminary requirements have established that the refabrication process should be accomplished with the minimum number of operations. Equipment should be of componentized-subassembly design with each of the component subassemblies removable and replaceable by simple crane and manipulator motions. Simplified processes and equipment are required for remote controlled operation.

The necessity of operating within an inert atmosphere, with process charges in the 10^4 curie range, and with hard, somewhat brittle, residual alloys, imposed further design requirements and limitations upon the selection of the process. Equipment should be totally replaceable for process flexibility.

Of several possible methods of producing a fuel pin, 0.1445 $\pm$ 0.001" diameter by 14 22 $\pm$ 1/32" long, precision casting offered the advantage of a short operational sequence, simplicity of equipment, and was not limited to the fabrication of ductile materials. Casting techniques when properly controlled do not orient the structure and thereby minimize one cause of radiation damage

Recently, the commercial production of precision bore glass tubing has been extended to the manufacture of fused quartz and high silica glass tubes to bore tolerances of $\pm$0.0005". Some grades of high-silica glass have softening points above 1500°C and will withstand over 1000°C

of thermal shock per millimeter of thickness. Glass molds may be pulverized away from the castings and, since the glass is inert to most acids, the valuable fuel residues may be separated from the pulverized glass by leaching. The glass, however, reacts rapidly with molten uranium and must be protected by means of a refractory coating.

The length to diameter ratio of 100:1 would not be easily obtained by gravity casting. Bottom gating was desirable to eliminate flow marks. Injection casting with the metal forced into the mold from the bottom was therefore indicated. Injection casting machines commercially available are complex mechanical machines casting molten metal into permanent molds by hydraulic action. For many reasons they were totally unsuited for the EBR-II fuel application.

A concept of gas pressure injection casting was developed which was essentially nonmechanical in nature. Very simply stated, the concept was based upon the possibility of supporting a column of molten metal in an evacuated tube, one end of which is submerged, by applying a pressure difference across the wall of the tube and between the exposed surfaces of the metal inside and outside the tube.

In the injection casting process for the production of EBR-II fuel pins, the U-5 w/o Fs alloy is melted under vacuum in a ThO_2-coated graphite crucible. The molds, in the form of high-silica glass (Vycor 7911) tubes closed at one end, are suspended open end down over the molten bath. During melting, the assembly of mold tubes is heated by resistance windings within the vacuum chamber. When the molten alloy has reached the selected casting temperature, the vacuum pumping system is isolated from the furnace chamber and the crucible is caused to rise, submerging the open tube ends. When the crucible reaches its uppermost level, the actuating ram trips a snap switch which opens the evacuated furnace chamber to an accumulator tank containing an inert gas (helium or argon) under pressure. The momentary pressure difference across the wall of the submerged tubes causes the molten alloy to rise into the tubes where it freezes. The crucible containing the remainder of the molten alloy is lowered in about 10 seconds after pressurization and while the metal in the crucible is still molten, but after solidification of the castings. Figure 4 shows a schematic representation of equipment to produce injection castings by the method outlined above.

It had appeared possible at first to cast as many as 100 fuel pins at one time; however, an analysis of the self-heating effects of the irradiated fuels indicated that concentric rows of castings in such numbers would be prohibitive due to the inability to cool the cast pins. This problem was solved by rearranging the geometric pattern and reducing the numbers of pins cast.

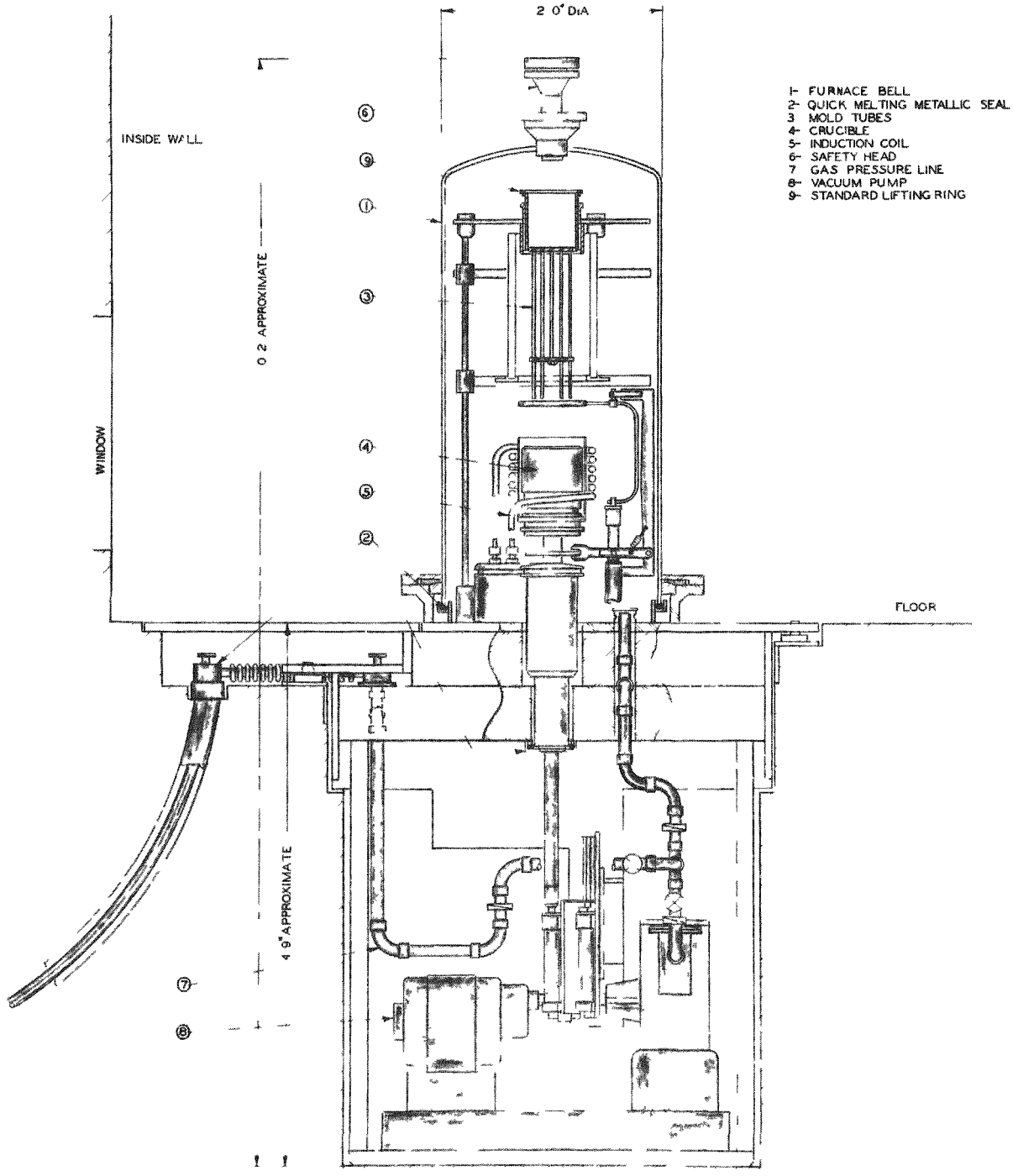

SCHEMATIC
INJECTION CASTING FURNACE

106-2874

Figure 4.

Figure 5 is a photograph of the prototype injection casting equipment which was employed to determine the parameters within which the casting technique must operate in order to produce acceptable castings. At this writing, the injection casting technique has been reduced to three areas of study: (1) length and diameter of castings; (2) surface condition of casting; and (3) weight of finished fuel pin (dimension and density). As a first consideration, the variables controlling the length of casting have been established as (a) melt temperature, (b) initial accumulator pressure, (c) pressurizing time, and (d) mold temperature. The surface condition of the castings has been tentatively attributed to the condition of the mold coating applied and, for purposes of controlling this variable, a coating consisting of finely divided ThO_2 suspended in an alcohol dispersion of colloidal graphite has been selected from the several that have been tried. Seventeen preliminary experimental runs are summarized in Table I, with an analysis of the length of casting.

The data and calculations presented in Table I were used to evaluate prior casting techniques and to project the operating parameters required to cast full length castings into the coated molds. After organization and classification, Figures 6, 7, and 8 were plotted, showing melt temperature, casting pressure, and time to arrive at final furnace pressure versus casting length. Consideration of the above data suggested the conditions for achievement of full length castings, 15" plus. These conditions were predicted based upon the above and were adjusted on four casts of U-5 w/o Fs alloy. The results of these tests are shown in Figure 9.

An analysis was made on the diameters of 78 castings. Each casting was measured on six diameters from top to bottom. It was found that more than 80% of the 608 measurements taken were within 0.1445 ± 0.0010". Furthermore, the extreme lower ends of the castings tended to exceed the 0.1445" upper limit. Cropping 3/4" from the lower ends removed the shrink cavity and also tended to bring the measurements in line with the specified results. Diametral variation was observed to be a function of the diameter of the molds into which the metal is cast and the regularity of the refractory coating film. A special pneumatic gage has been ordered for measurement of the tube bore and work is continuing upon coatings.

A number of refractory coatings have been tried, including coloidal graphite, magnesium-zirconate, calcia, thoria, uranium oxide, zirconia, and combinations of the above with colloidal graphite. The most satisfactory of these has been a dispersion of thoria in a dilute colloidal graphite-ethyl alcohol suspension. Thirty to forty per cent of the solid material can be finely divided ($40\,\mu$) ThO_2. This material was doctored onto the inside of the tubes by means of a pipe cleaner swab. The alcohol was

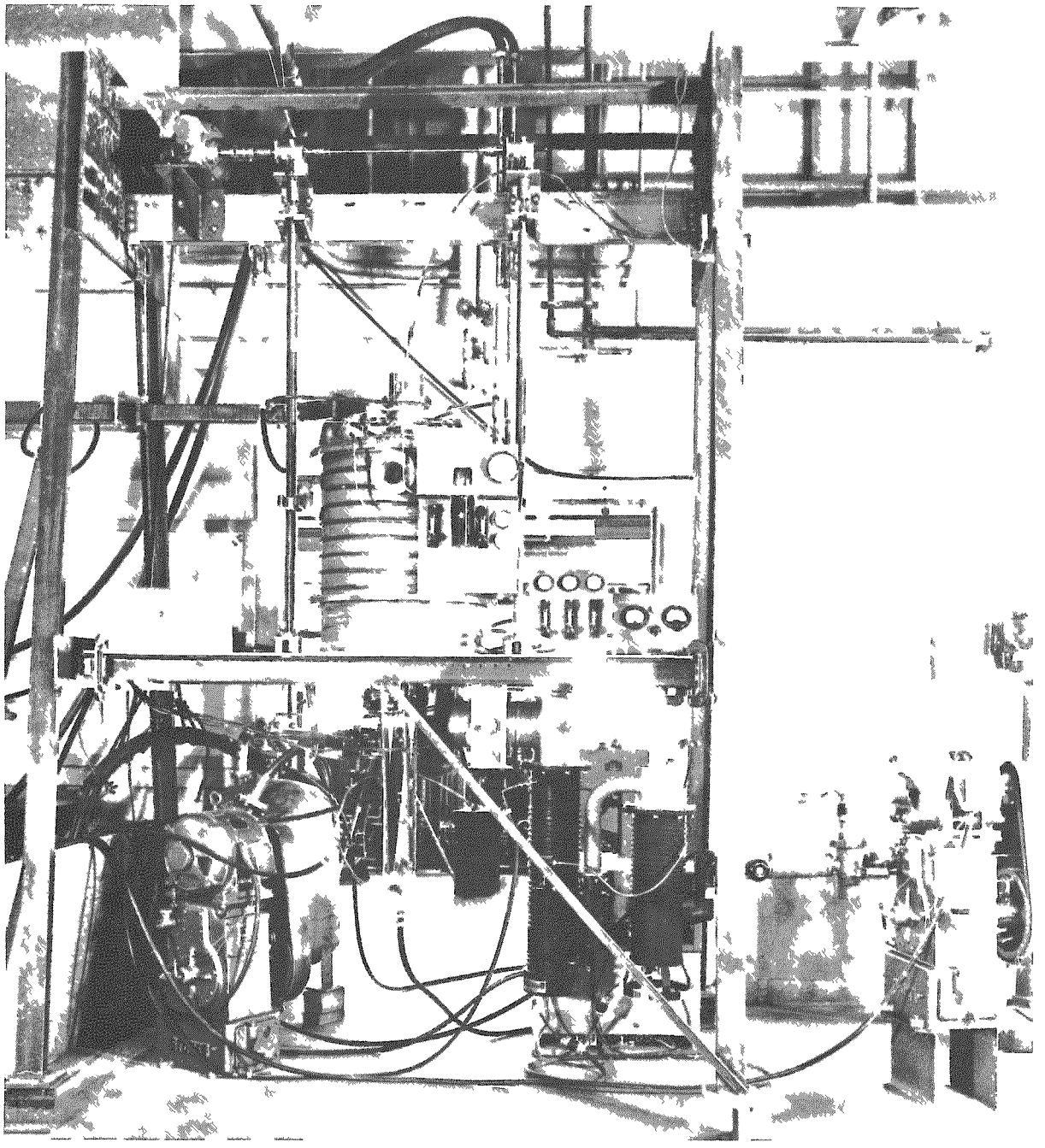

106-2495

Figure 5. Prototype of Injection Casting Equipment

TABLE I

Data On Seventeen Experimental Runs To Study Effects Of Casting Variables On Lengths Of Castings

Melt No.	Melt Temp. (°C)	Operating Variables			Statistical[1]		
		Log Mean Mold Temp. (°C)	Initial Casting Pressure (psia)	Pressurizing Time (sec)	n	$\bar{x}$ (in.)	s (in.)
2A7	1275	400	35	1	5	13.1	1
1C3	1275	380	40	1	--	12.0	--
1A9	1275	360	45	1	10	12.3	3.0
1A10	1275	360	75	1	15	16.8	0.8
1C5	1275	360	75	5	15	10.6	1.1
4A2	1275	370	75	5	5	12.0	1.0
2C2	1275	320	75	3	15	13.0	1.6
1C2	1265	250	55	1	15	14.1	3.3
2C3	1350	400	75	5	20	10.4	1.0
L381-2	1285	610	75	3.5	15	13.8	1.0
5A3	1285	460	75	4	18	12.0	3.0
5A4	1285	580	75	3.5	13	15.8	1.8
5A2	1300	340	73	5	4	15.5	1.5

[1] n = Number of castings

$\bar{x}$ = Average length of casting

s = Standard deviation of length distribution

removed by oven drying at low temperature. Bake-out under vacuum 400° to 500°C prior to casting was very important to eliminate the last traces of moisture. It was possible by this method to produce very smooth, thin, adherent coatings.

Enriched Uranium-Fissium Specimens: Two casts of 25 pins each were made using 10% U^{235} enriched U-5% Fs alloy to provide both full size fuel elements and small samples for in-pile irradiation studies. The computed composition and casting conditions are shown in Table II.

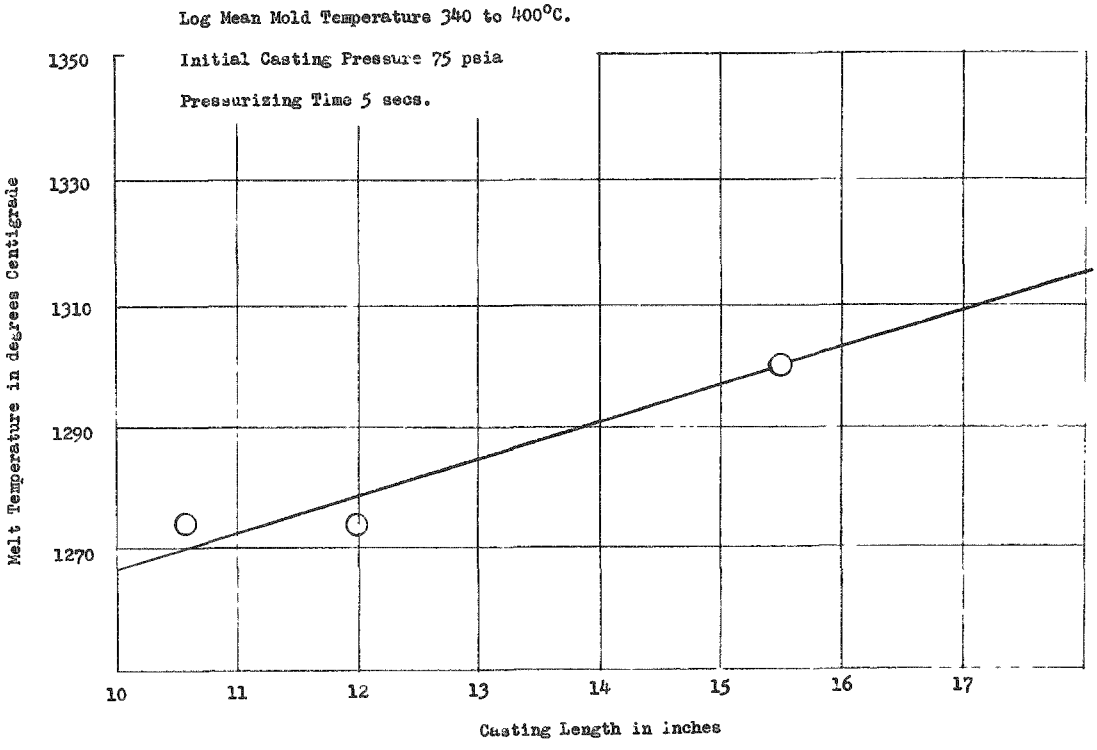

106-3158 Figure 6. Plot of Melt Temperature in °C. versus Casting Length in inches

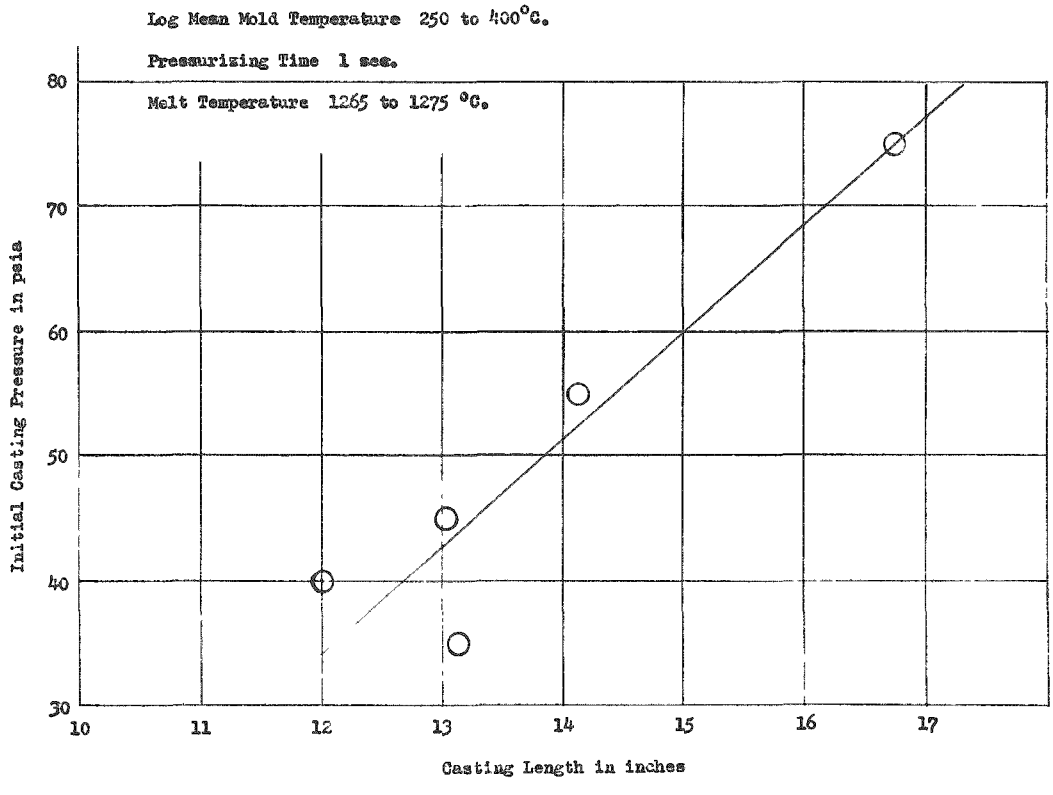

106-3157 Figure 7. Plot of Initial Casting Pressure in psia versus Casting Length in inches.

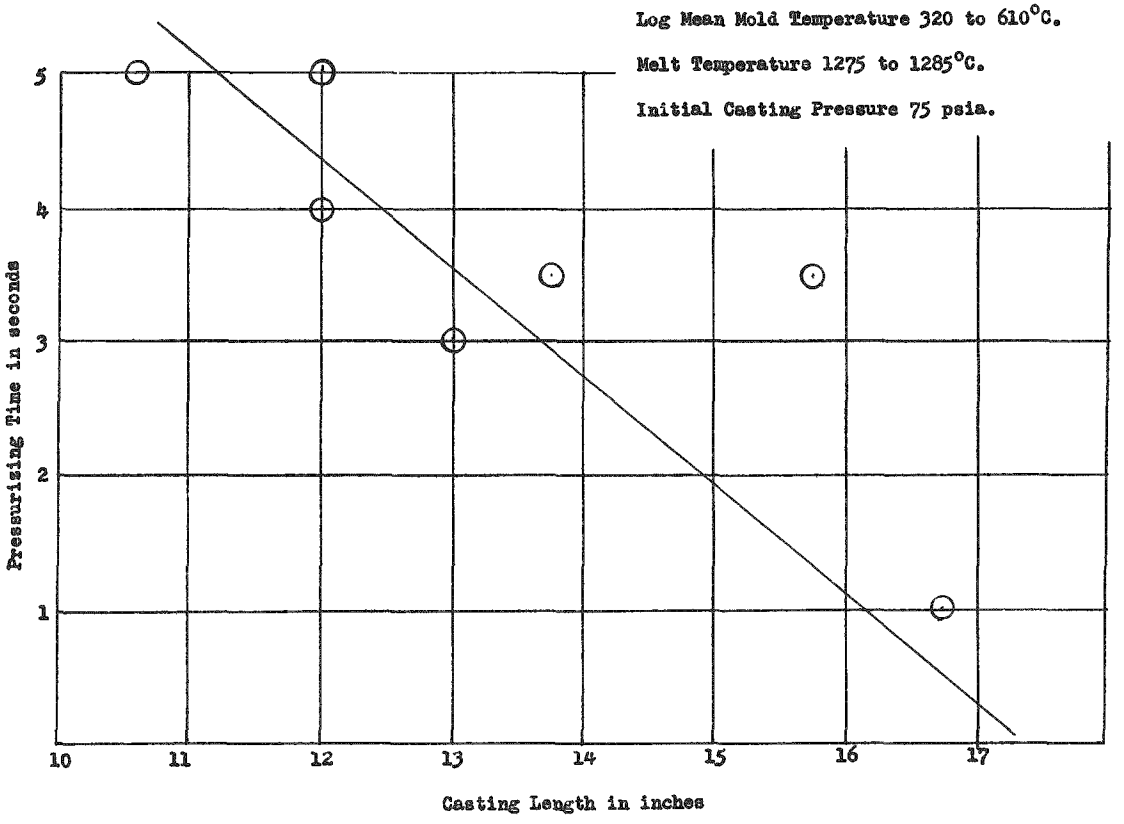

106-3156 Figure 8. Plot of Pressurizing Time in secs. versus Casting Length in inches

Casting No.	Melt Temp. °C.	Initial Casting Pressure psia	Pressurizing Time sec.
3C1	1320	53	3
3D2	1320	42	2
3D3	1325	45	2
4D2	1325	45	2

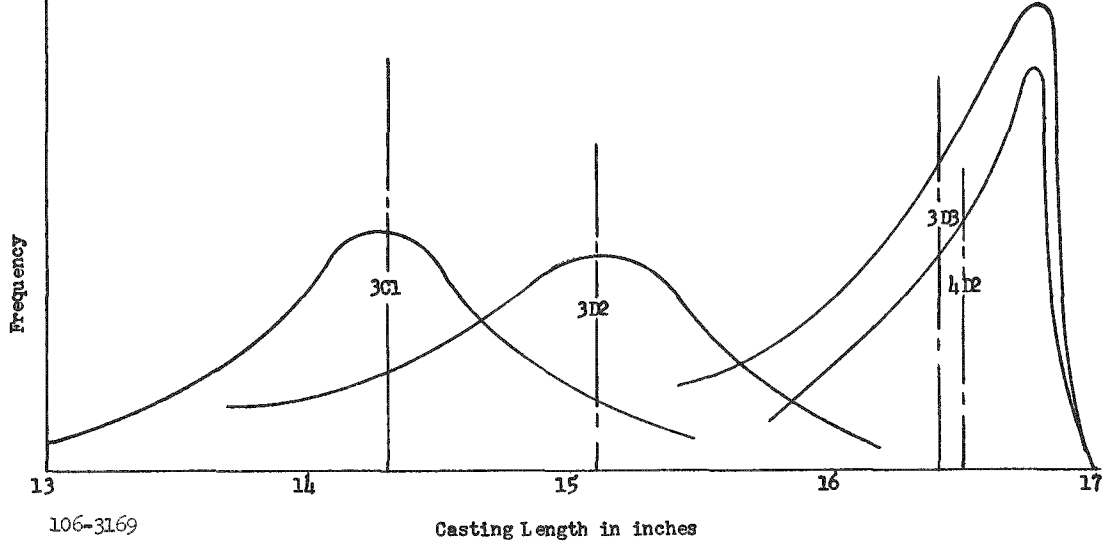

106-3169

Plot of Individual Casting Length Frequency Versus Casting Length in inches for Casting Conditions as Noted.

Figure 9.

TABLE II

Charging And Casting Data. Injection Cast Heat 1E2

Total weight of metal charged: 2849.796 g

Calculated Composition of Charge (w/o)

Zr	Nb	Mo	Ru	Rh	Pd	U^{235}	U^{238}
0.06	0.01	2.48	1.97	0.29	0.19	10.00	Balance

Temperatures (°C)

Metal (when cast)	1330
Molds, Top	334
Bottom	600

Pressures

Initial Tank	45 psia
Final Furnace	25 psia
Pressurizing Time	2 seconds

Casting Length, Average (in.)	16.04
24 Castings Over	15.00
1 Casting	13.44
Castings Weight	1930.71 grams
Crucible Heal (Remelt)	919.07 grams

A complete tabulation of weights, densities, hardness, and dimensions of 25 pins from the first enriched batch (1E2) is presented in Table III to indicate variance. A photograph of the pins is shown in Figure 10. Figure 11 shows surfaces produced by the graphite-thoria mold coating.

Remote Control Process: The development of an injection casting method has resulted in a very simple operational sequence consisting of (1) injection casting, (2) mold removal, (3) shearing to length, (4) weighing, and (5) dimensional inspection. A flow diagram of the process is shown in Figure 12.

TABLE III

Properties And Dimensions Of Heat Number 1E2

Pin No.	Weight (grams)	Diameter $\bar{d}$ (inches)	Length (inches)	Hardness, R_C		Density (g/cc)
				Top	Bottom	
1	66.245	0.1442	14.22	46	44.5	18.286
2	69.130	.1415		46	46.5	18.241
3	66.849	.1438		44.5	47	17.747
4	68.832	.1439		43.5	43.5	18.271
5	69.248	.1440		46.5	43	18.276
6	69.445	.1440		46.5	46	18.276
7	69.191	.1445		45	42.5	18.193
8	69.415	.1440		45	43.5	18.279
9	68.843	.1440		42.5	42	18.287
10	69.345	.1439		46.5	44	18.282
11	69.307	.1443		45.5	47	18.301
12	68.157	.1440		44	43.5	18.034
13	69.333	.1440		46.5	40.5	18.279
14	67.027	.1441		46	46.5	17.764
15	69.327	.1440		44.5	44	18.288
16	69.523	.1444		45.5	41.5	18.283
17	69.490	.1440		46	45.5	18.290
18	68.824	.1439		44	43	18.079
19	69.201	.1439		43.5	45.5	18.304
20	69.279	.1442		45	45.5	18.297
21	69.094	.1441		43.5	46.5	18.291
22	69.011	.1443		46	46	18.183
23	68.491	.1443		46.5	47.5	18.020
24	(67.298)	.1445	(13.94)	45	46.5	18.096
25	(58.603)	0.1445	(12.00)	43	41	18.294
Average	68.977	0.1441	---	45.0	44.5	18.198

Note: Indicated average weight applies to full length pins only.

An injection casting machine has been designed for remote operation mock-up and is shown in Figure 13. The vacuum system and accumulator tank will be located in a sealed, lightly shielded container outside the process cell wall.

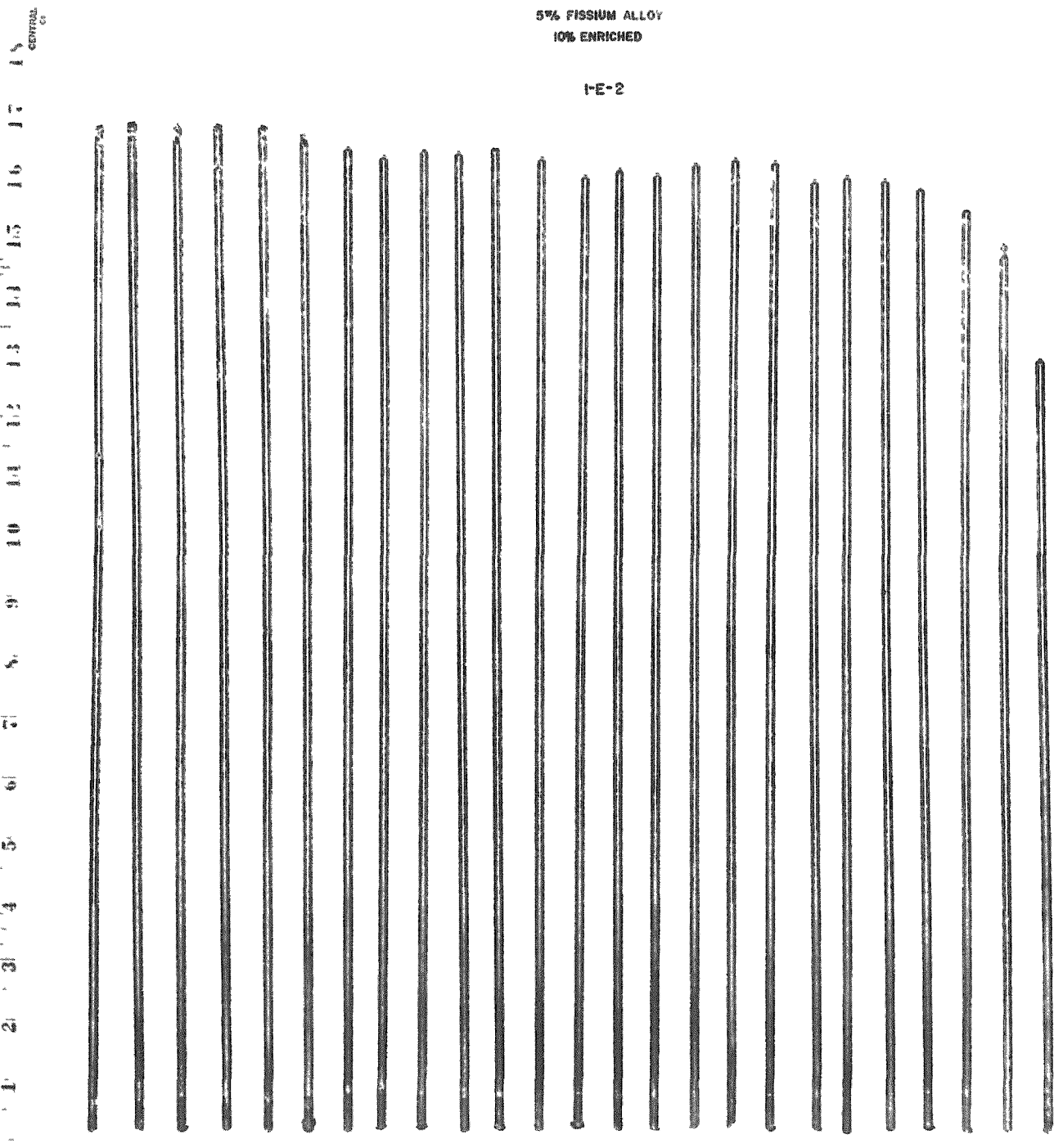

106-3155

Figure 10. Fuel Pins Produced in Heat #1E2

10 w/o U^{235} enriched U-5 w/o Fs alloy

04X

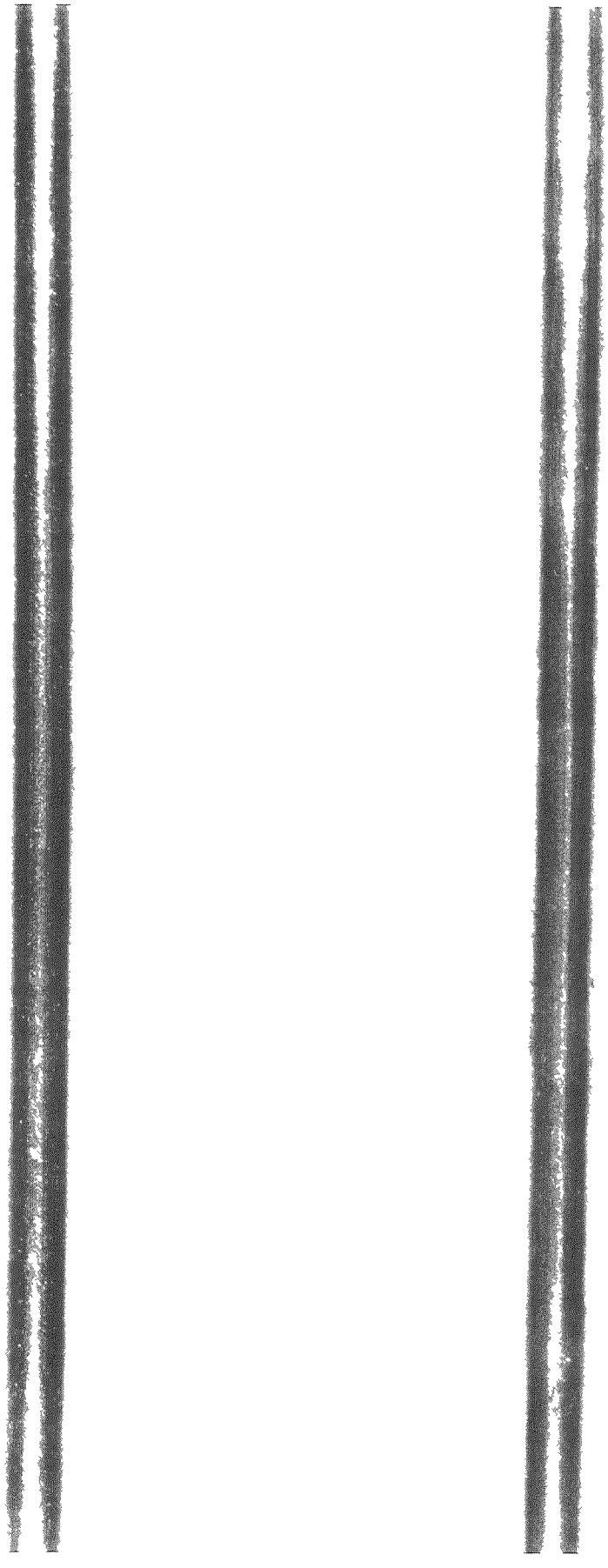

106-3154 3-X

Figure 11. Fuel Pins, Heat 1E2, Showing Surface Conditions

Figure 12.

FLOW DIAGRAM OF EBR II FUEL REFABRICATION PROCESS

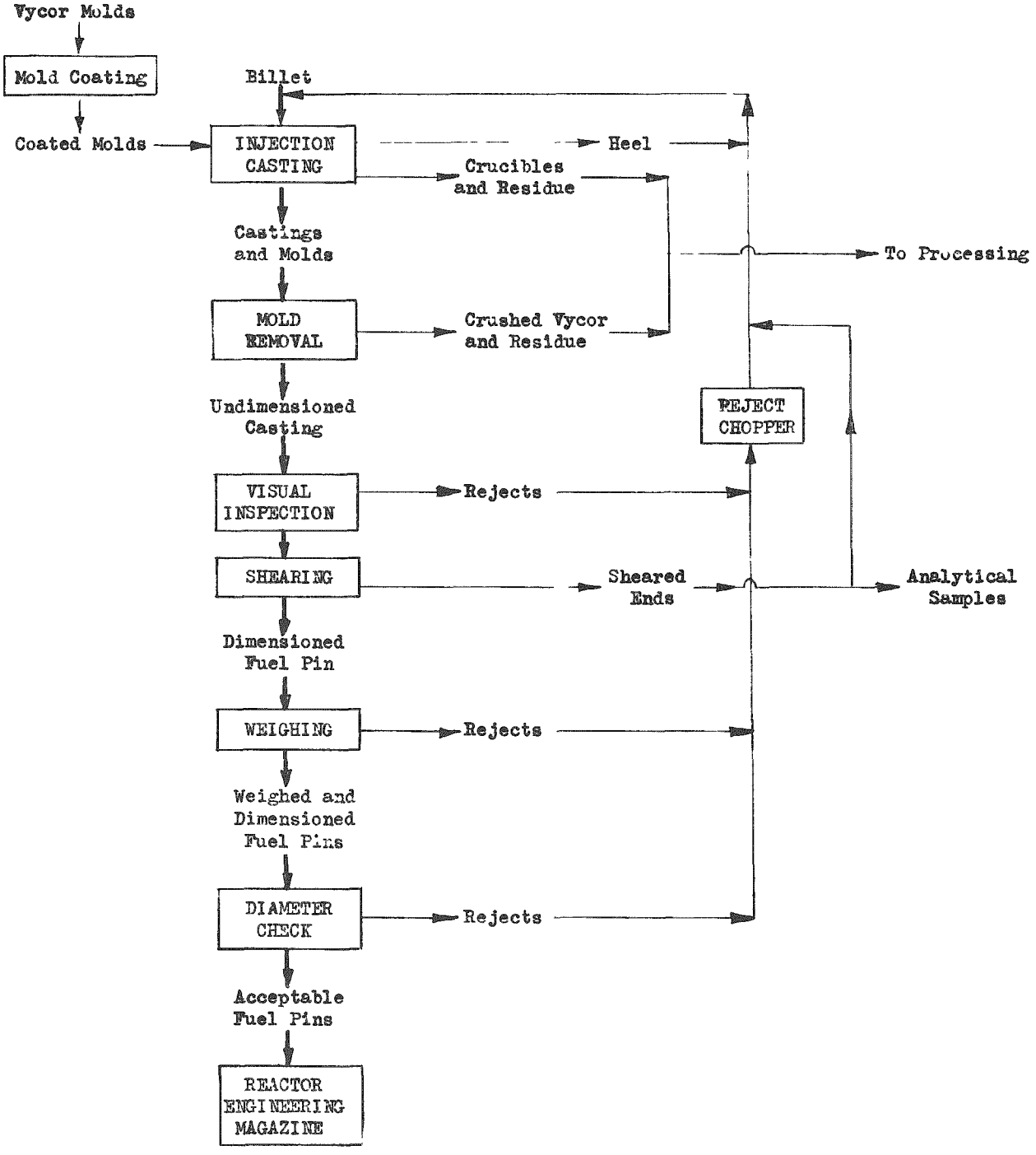

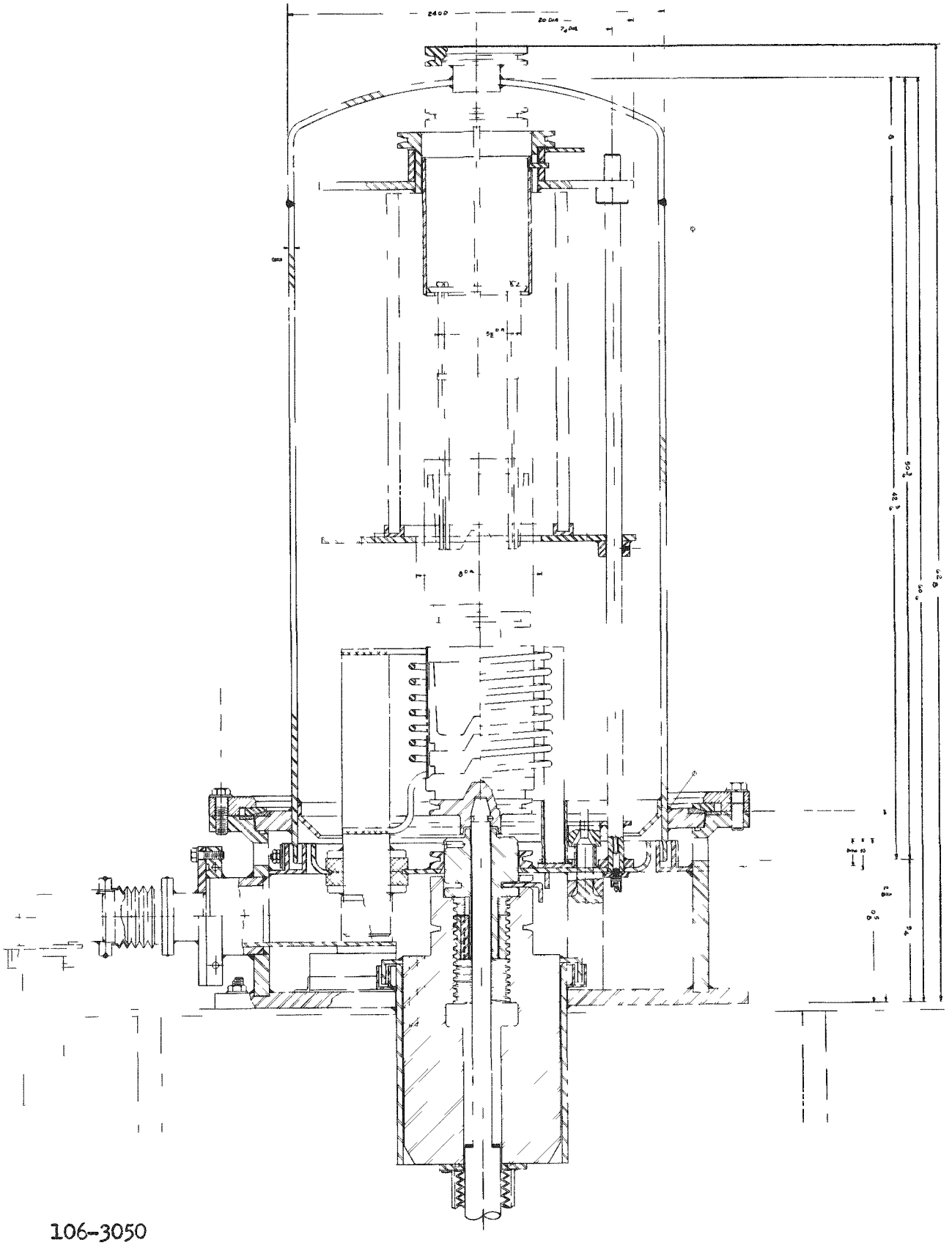

106-3050

Figure 13. Injection Casting Furnace for Remote Control Cell Mock-up

The glass molds have been successfully removed by passing the tubes and castings between a pair of concave, toothed rolls, which break the glass into fragments but allow the casting to pass through.

It is proposed that shearing to length, weighing and inspection be carried out on a simplified transfer mechanism. Preliminary designs have been worked out on three transfer mechanisms using the inclined plane, the rotary table and the belt. The simplest is the inclined plane down which the castings roll from station to station.

3. Properties of Uranium-Plutonium-Fissium Alloys (R. J. Dunworth)

A Vycor tube furnace, 4" in diameter, was constructed to make EBR-II fuel pins by the injection casting method. Some test pins of uranium and U-10 w/o Fs were cast successfully into the Vycor tube molds. The graphite crucibles were coated with a magnesium-zirconate wash, and the Vycor tubes were coated with an Aquadag wash. Since both the crucible and the mold were attacked by molten uranium, thoria powder (about 30 volume per cent) was added to both washes. The corrosion was stopped or was considerably reduced by this addition. The solidus temperature was measured approximately for the following two alloys: U-10 w/o Fs at 1000°C, and U-20 w/o Pu-10 w/o Fs at 930°C. These values are very close to solidus temperatures reported for U-5 w/o Fs and U-20 w/o Pu, respectively.

III. ARGONNE LOW POWER REACTOR - ACTIVITY 4202

1. Fuel Plate Evaluation (R. A. Noland, D. E. Walker)

Evaluation of a small number of the subject fuel plates has been in progress during most of the past quarter. The plates were made by commercial suppliers operating under development contracts. They were fabricated by hot roll cladding cores of aluminum-uranium alloy with M-388 aluminum alloy on all sides. Nickel additions were made to the core material to provide additional corrosion resistance to high temperature (290°C) water. Boron in amounts approximating 0.5 w/o was also present in the cores. Some of the plate cores were made by a powder metallurgical technique, namely, cold pressing followed by hot (600°C) rolling. The remainder were produced by melting, casting, and hot rolling. Among the items for which these plates are being evaluated are:

1. Resistance of cladding and core to corrosion by 290°C high-purity water.
2. Continuity of bond.
3. Conformity (external) with specified dimensions.
4. Surface appearance: presence of laps, seams, scratches, pits, etc.
5. Cladding thickness.
6. Core composition and homogeneity.
7. Core shape and its symmetry in respect to the entire plate.

IV. ADVANCED ENGINEERING AND DEVELOPMENT - ACTIVITY 4530/4540

1. Examination of EBR-I, Core II Meltdown

a. Physical and Metallurgical Changes in the Damaged EBR-I Core (J. H. Kittel)

The damaged EBR-I, Core II was disassembled during the previous quarter. From observations and photographs made during disassembly operations (Figures 14 through 18), and from chemical, metallographic, and density measurements, it has been possible to reconstruct the probable physical structure of the core after the meltdown. Figure 19 shows a preliminary drawing of the various areas found in the core, which varied widely in density because of the development of a porous structure. Presumably, the porosity resulted from NaK vapor in the molten fuel alloy.

b. Metallographic Examination of EBR-I Meltdown Specimens (F. L. Brown)

The investigation of the EBR-I, Core II meltdown included metallographic examination of material from five zones of the fused core. The specimens retained for examination are shown in Figure 20, in order of increasing density, and were referred to as follows: (1) coarse sponge material; (2) fine sponge material; (3) eutectic; (4) high-density material; and (5) undissolved fuel slugs. Two zones in particular were noted as having a high degree of porosity. Examination of sections at higher magnification disclosed porosity in all specimens except in the partially dissolved fuel, as shown in Figure 21. NaK alloy, entrapped in the pores, stained and discolored specimen surfaces during grinding, causing some difficulty in the preparation procedure.

Presupposed alloying of the uranium fuel with the stainless steel jacketing material and subsequent eutectic melting at a temperature below the melting point of uranium was confirmed by the microstructures. As shown in Figure 22, significant amounts of eutectic were present in each zone. Constituents observed were similar in appearance to the delta (U_6Fe) and epsilon (UFe_2) phases in the uranium-iron system.

2. Graphite-UO_2 Fuel Elements for the TREAT Reactor (J. H. Handwerk, R. C. Lied)

The proposed TREAT reactor is to be fueled with UO_2 dispersed in graphite. The composition of this fuel has been suggested as either 1 or 2 w/o UO_2 and the balance graphite. The UO_2 will be dispersed in the graphite, and the graphite compacts will be either carbonized or graphitized depending on the fabrication tolerance which can be held.

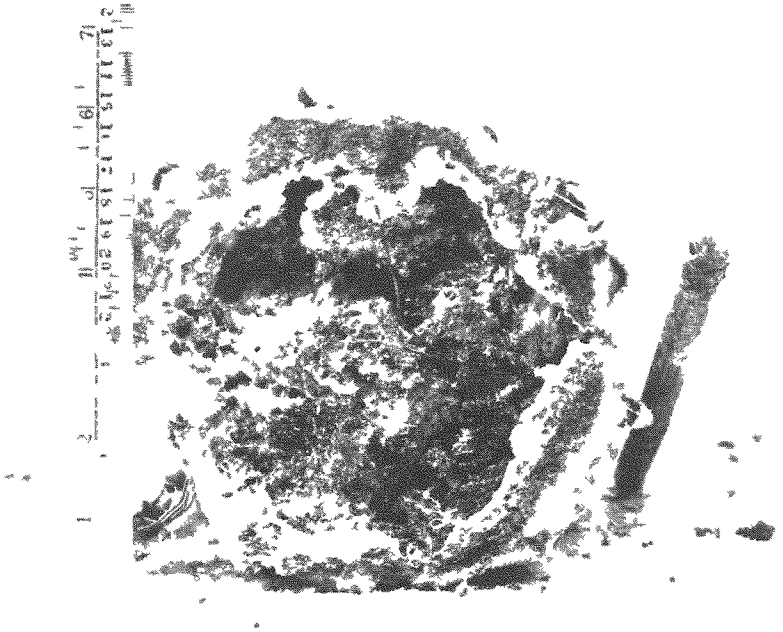

106-3095

Figure 14.

Cross-Section at Midplane of Damaged EBR-I Core, Illustrating Range of Porosity.

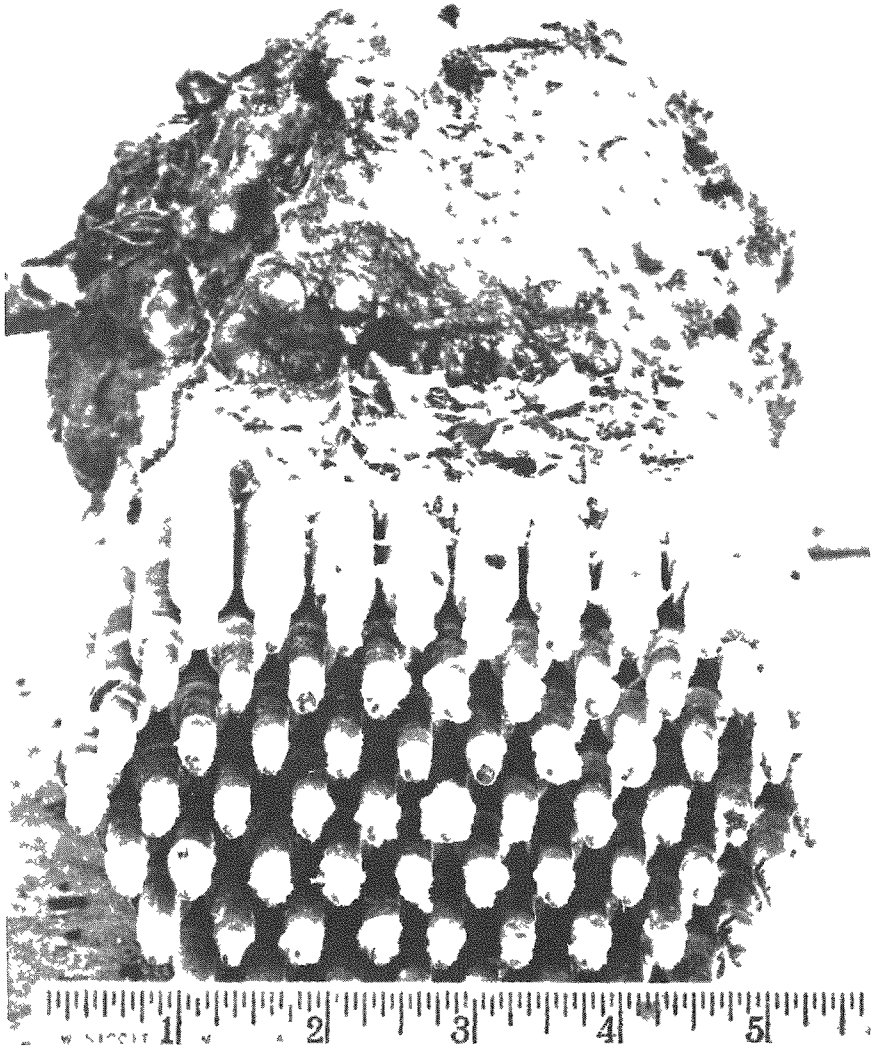

106-3100

Figure 15.

Bottom of Damaged EBR-I Core, after Removal of Part of the Lower Blanket.

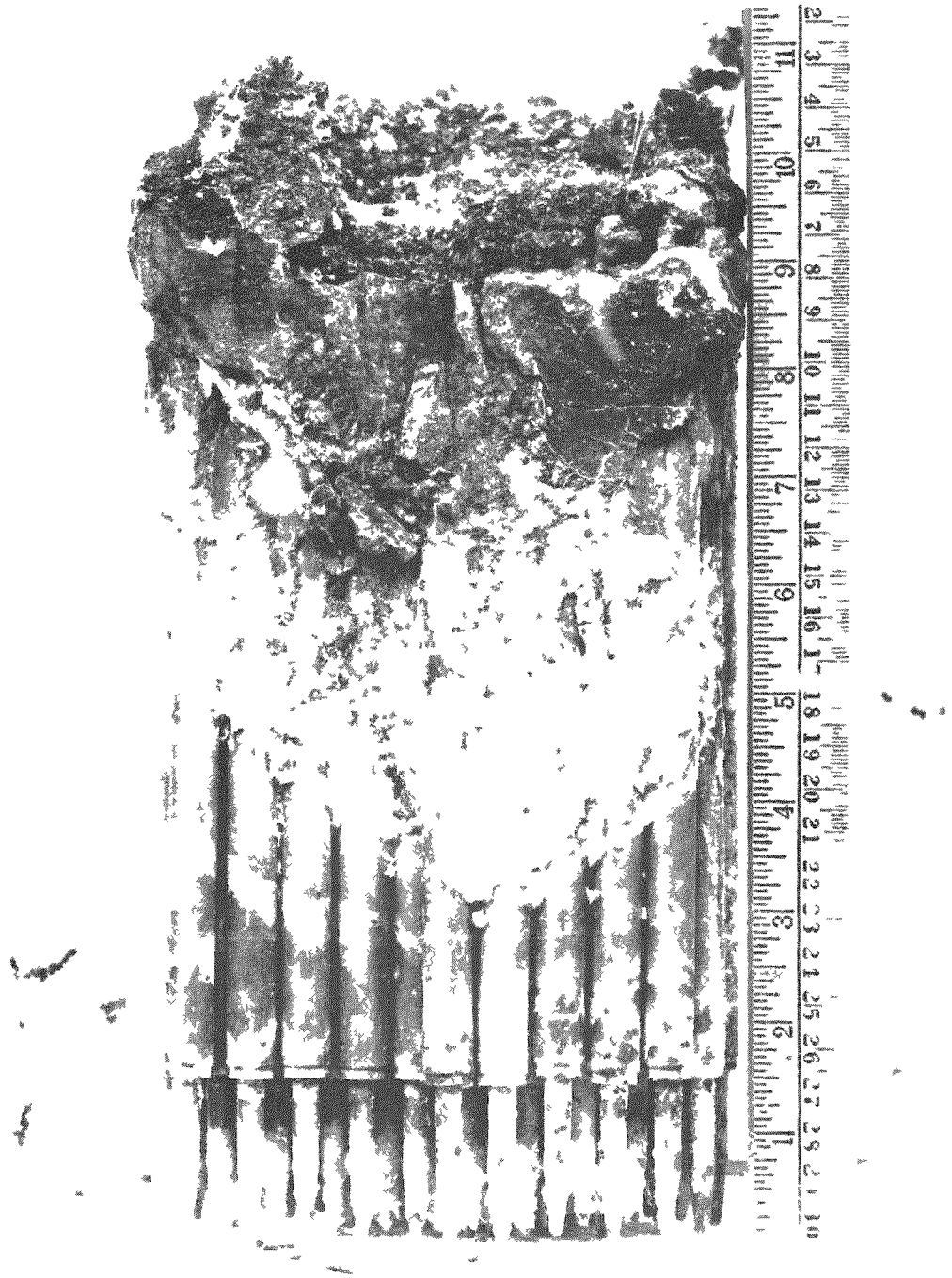

106-3110

Figure 16.

Vertical Cross-Section of the Lower Half of the Damaged EBR-I.

106-3105

Figure 17.

Upper Blanket Rods from the Damaged EBR-I, Illustrating Upward Flow of Molten Fuel Alloy.

106-3106

Figure 18.

Partially Dissolved EBR-I Fuel Slugs, Embedded in Solidified Fuel Alloy.

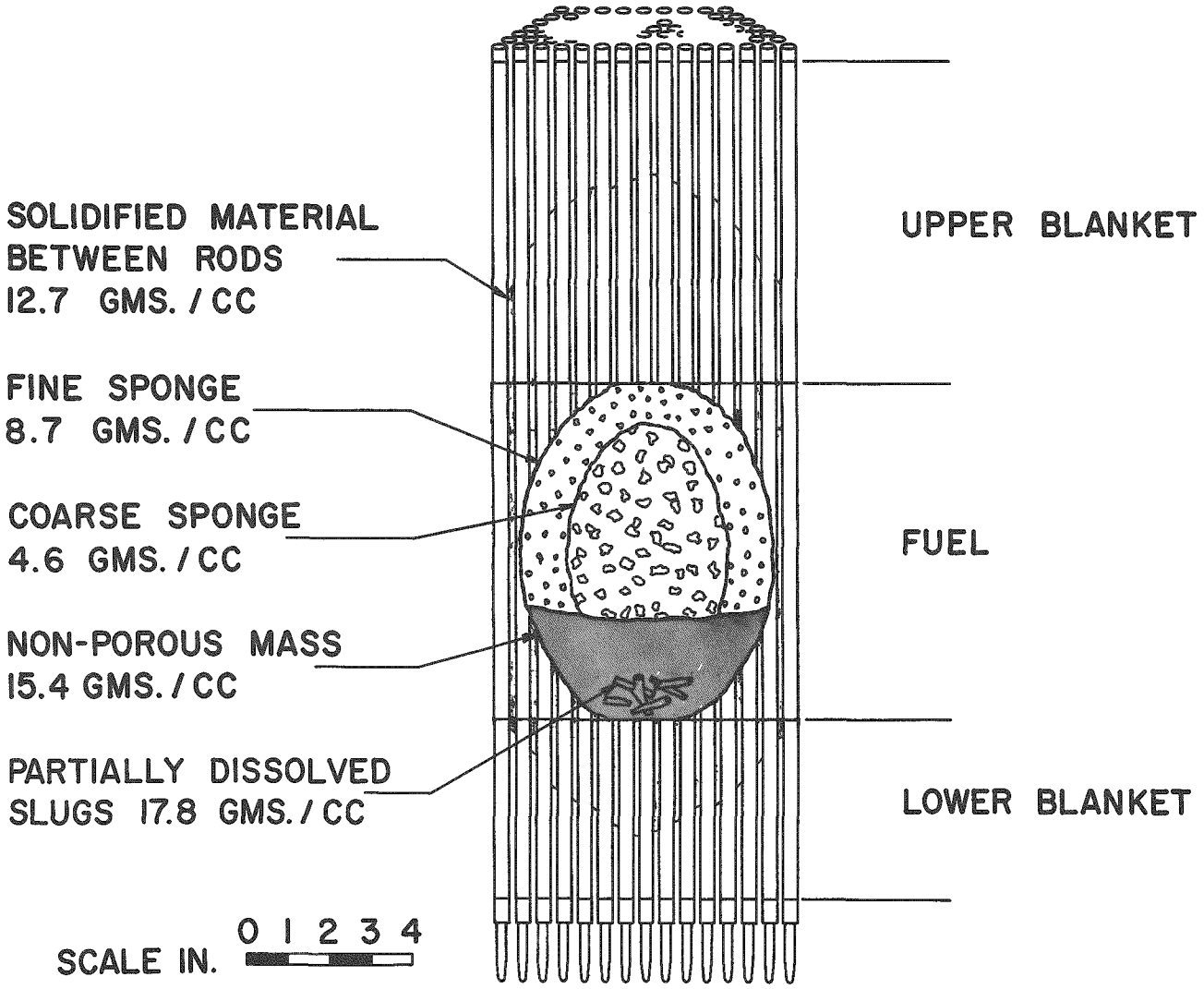

Figure 19.

VERTICAL SECTION THROUGH DAMAGED EBR-I CORE

Figure 20. Specimens from EBR-I, Core II Meltdown.

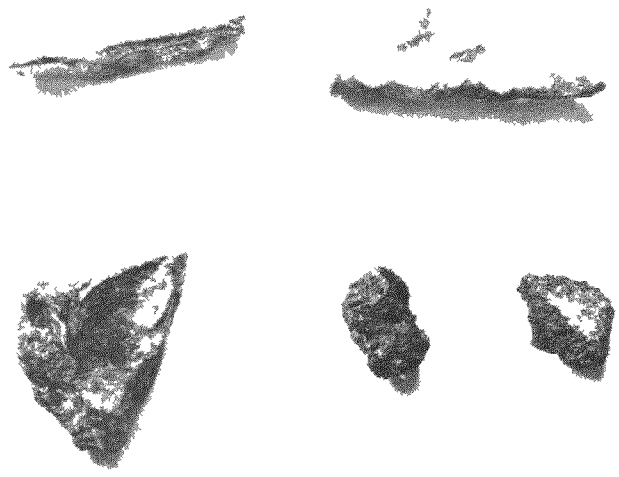

Macro 21240 1-X

Top: Left - Eutectic
Right - Undissolved Slug

Bottom: Left - High Density
Middle - Coarse Sponge
Right - Fine Sponge

A preliminary study of organic bond materials for graphite powder has been initiated. From this study it appears that graphite powder, bonded with organic resins such as Bakelite or furfural alcohol, can be readily fabricated. This study will continue in an effort to determine the best bond material.

3. Nondestructive Testing (W. J. McGonnagle, W. N. Beck, C. J. Renken, Jr.)

a. Ultrasonic Tests of Cylindrical Castings

A transmission test was conducted on 14 cylindrical uranium castings which are to be used in the manufacture of EBR-I, Mark III fuel elements. The castings measured approximately 11" in length and 2" in diameter. A transmission technique at a frequency of 1 megacycle was successfully used in the determination of shrink and porosity.

Figure 21. Porosity in Meltdown Areas.

21-a. Coarse Sponge

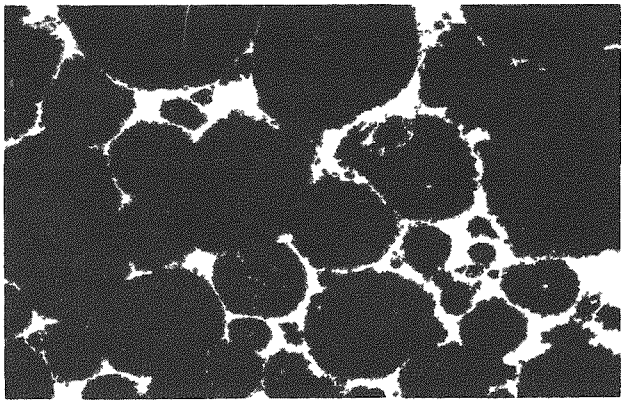

Micro 21237 50-X

21-b. Fine Sponge

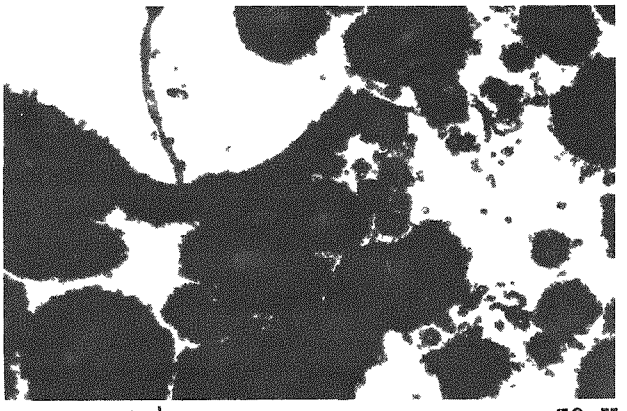

Micro 21234 50-X

21-c. Eutectic

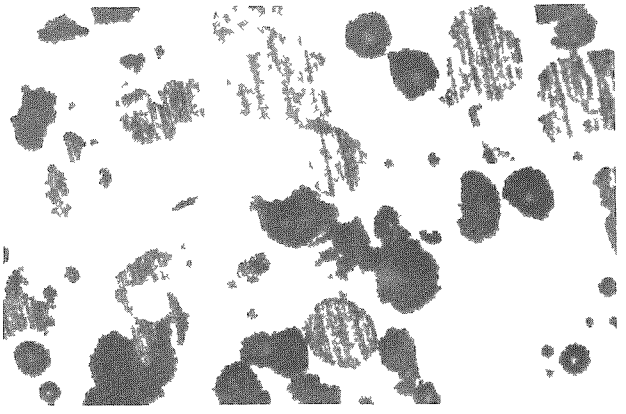

Micro 21231 50-X

21-d. High Density

Micro 21224 100-X

21-e. Undissolved Fuel Slug (left) and Adjoining Material

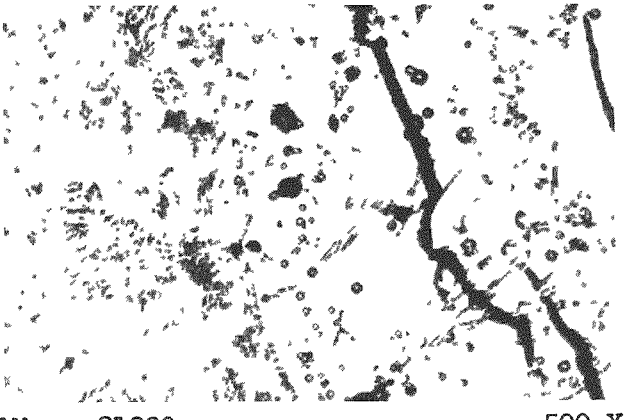

Micro 21230 500-X

Figure 22. Eutectic Areas in Meltdown Specimens.

22-a. Coarse Sponge

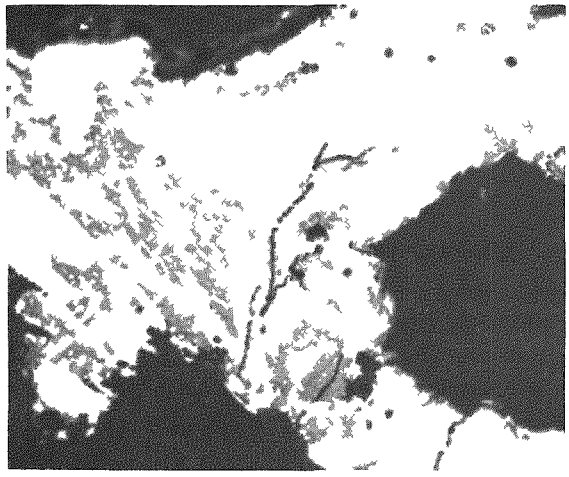

Micro 21238 431 DPH 500-X

22-b. Fine Sponge

Micro 21236 446 DPH 500-X

22-c. Eutectic

Micro 21233 456 DPH 500-X

22-d. High Density

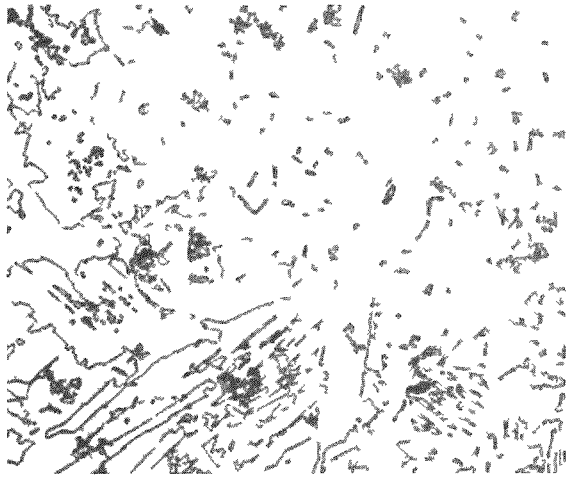

Micro 21225 444 DPH 500-X

22-e. Undissolved Slug (left) in High Density Material

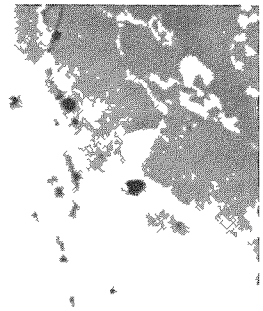

Micro 21229 301 DPH 384 500-X

b. Ultrasonic Fluoroscopy Unit

The necessary equipment is being procured for the completion of an ultrasonic fluoroscopy unit. In this particular design, two 4" x 4" barium titanate transducers are used. The silver coating on one of the transducers is divided into a 196-segment mosaic. The holders for the transducers have been made and the electrical connections to the mosaic completed. In addition to attempting a synchronized video screen image of the ultrasonic energy, a multiple neon light mosaic will be considered. By this last mentioned method, the output of each segment of the mosaic will be amplified and made to operate a miniature neon light. A battery of such lights will constitute the raster.

c. Eddy Current Testing

Development was continued on a dual channel, selective eddy current testing system for the measurement of the thickness of one metal clad on another. This system is able to undertake tasks which have previously been impossible for eddy current methods because of the effect of probe-to-metal spacing. Measurements of the average cladding thickness are made over an area as small as 0.02 square inch, which is a considerable improvement over other methods of nondestructively measuring cladding thickness. A further advantage is that it is possible to inspect the subsurface layers of a metal for voids, inclusions, etc., without interference from surface conditions, since the instrument is capable of automatically compensating for conditions on the surface. This system is designed for production applications. Present plans are to use it to measure the cladding thickness on the EBR-I, Mark III fuel elements.

The permeability of nickel is influenced by the amount of cold work to which the metal has been subjected. Preliminary studies were made to determine the feasibility of directly measuring the amount of cold work in nickel by means of eddy current methods. Specimens were stressed in a testing machine and the permeability was indirectly measured by an eddy current instrument. Diagrams much like the familiar stress-strain curves resulted which showed the elastic limit, yield point and rupture. There is a possibility that these methods may be useful in determining directly the internal stresses in nickel and possibly some steels.

4. Corrosion Properties

a. Dynamic Corrosion Test Facility (S. Greenberg, W. E. Ruther, J. E. Draley)

A high-temperature, high-pressure dynamic corrosion test facility has been under consideration since early April, 1956. Active design started during late Spring of 1956.

Construction and procurement of components has been completed and the facility has been assembled and tested. Testing of samples is expected to begin in the next quarter.

Design conditions of the facility are:

Maximum temperature:	360°C
Maximum pressure:	3000 psia
Maximum flow rate:	20 - 30 feet/second (depending on number of samples tested).

Important features of this facility, in addition to the maximum design conditions, include:

1. Pressurization by means of a piston pump and back-pressure regulator instead of the usual surge tank. This procedure allows for more accurate control of dissolved constituents in the water. In addition, the pressurizing system doubles as the means for adding make-up solution.

2. Sample sections are removable (and therefore replaceable) while the system is at operating temperature and pressure. This will greatly reduce down time. In addition, the valving arrangement necessary for this operation permits the use of four different velocities simultaneously.

b. Corrosion-Resistant Uranium Alloys (S. Greenberg, J. E. Draley)

In an effort to show the existence of a cathodic second phase in as-quenched uranium alloys, low-current, short-time plating of copper on samples is being done. To date, results have been erratic. Plating can be made to take place nonuniformly, but results are not readily reproducible. Study of the variables which affect plating behavior will continue.

c. Corrosion-Resistant Aluminum Alloys (W. E. Ruther, J. E. Draley)

The emf of a pH-sensitive electrolytic cell was measured at elevated temperatures (to 300°C) using dilute hydrochloric and dilute perchloric acids as pH standards. A small autoclave was modified to supply one insulated electrical connection, a bayonet thermocouple, and a method of introducing hydrogen gas.

The cell used to measure the pH was platinized platinum (H_2) versus a silver-silver iodide electrode. The two electrodes were separated by a diffusion barrier made from a Vycor tube with a bead of Pyrex fused in the bottom. On cooling, such a tube develops fine leakage paths due to the

differential contraction of the glasses. A supporting electrolyte of 0.01 molar solution of potassium iodide was used in both compartments. The bayonet thermocouple (jacketed in Vycor for electrical insulation) was immersed in the solution under test.

The separation of the two electrodes is necessary since silver ion is reduced to silver metal by the hydrogen gas. This reaction takes place rapidly only at the platinized platinum. The accumulation of metallic silver on the platinum prevents the desired operation of the platinum as a hydrogen electrode. For the same reason the experiments were performed as quickly as possible. The total pressure within the autoclave was adjusted to 200 psig hydrogen in excess of the water vapor pressure at each temperature.

To standardize the apparatus, solutions of hydrochloric acid made up to pH 3, 4 and 5 were tested. The emf-temperature curve obtained with pH 4 hydrochloric acid was rechecked with pH 4 perchloric acid solution; good agreement was obtained.

The solution of interest, phosphoric acid, was then tested. On the HCl standard the pH 3.5 phosphoric acid (room temperature) had a pH of 3.75, and the pH 4.5 (RT) phosphoric acid had a pH of 4.77 at 290° C.

The purpose in making these measurements was to have a basis for separating the effects of anions and pH in the high-temperature corrosion of aluminum alloys. Accordingly, a corrosion test (alloy M-388) has been started in which the pH at 290° C is equivalent to pH 4.5 H_3PO_4, but whose phosphate concentration (NaH_2PO_4) is equivalent to pH 3.5 (RT) H_3PO_4. Also, another test has been started in which the pH at 290° C is equivalent to pH 3.5 H_3PO_4 (RT) (using H_2SO_4), but the phosphate concentration is equivalent to pH 4.5 (RT) H_3PO_4. The results of these corrosion tests (coupled with a knowledge of the corrosion rates in pH 3.5 and pH 4.5 H_3PO_4 solution) should present a qualitative picture of the relative importance of phosphate and hydrogen ions as inhibitors at 290° C.

Thermal Stability of H_3PO_4: A boiling experiment was performed to give preliminary information as to whether thermal decomposition or volatility would complicate the use of phosphoric acid solution in boiling reactors. An electrically heated stainless steel autoclave, 6" I.D. x 18" tall, was half filled with solution and 2 kw of heat supplied. At temperature (252° C, 600 psia) thermal equilibrium was established by bleeding and condensing the steam at the rate at which it was produced. The condensed steam was tested for pH and resistivity. This thermal equilibrium condition was maintained for about 30 minutes. At the end of this period the steam bleeding was stopped and the autoclave was maintained

at 250°C for an additional 4 hours. This was done to see if possible thermal decomposition of the phosphoric acid produced any volatile components. The steam was again bled at the equilibrium rate to distill these components if present. The results of the H_3PO_4 experiment are presented in Table IV.

TABLE IV

Condensate from pH 3.5* H_3PO_4 (250°C, 600 psia).

Test	Rate (lb/hr)	pH	Specific Resistance, ohm-cm (20°C)
Initial Equilibrium	3.6	5.7	1,300,000
After $4\frac{1}{2}$ hours at 250°C	3.6	5.7	1,300,000

* Measured at room temperature

A previous 1-hour run with distilled water produced a gradual cleanup of the system, with a terminal value of 450,000 ohm-cm specific resistance and pH of 5.5. Measurements of the first distillate with the H_3PO_4 solution showed essentially these same numbers. Within 15 minutes the specific resistance had exceeded 1 megohm, indicating that the cleanup was completed. For the next 15 minutes the values shown in the table for initial equilibrium were obtained.

The data indicate that the relative volatility of H_3PO_4 is very low under these operating conditions and that thermal decomposition to volatile products does not occur in this length of time.

Unfortunately, the autoclave available did not adequately represent a scale-down of EBWR. For example, at 60,000 lb/hr, the EBWR has a steam liberation rate in the vessel of about 50 pounds per minute per square foot of water-steam interface. The autoclave used provided a rate of only 0.3 in the same units. Due caution should therefore be used in extrapolating the boiling autoclave data to EBWR.

d. Corrosion of Magnesium (W. E. Ruther, J. E. Draley)

Due to the possible use of magnesium as a cladding material in a new reactor (Mighty Mouse) a few preliminary tests have been made with distilled water in small nonrefreshed autoclaves. The results are presented in Table V.

TABLE V

Corrosion of Magnesium

Temperature (°C)	Time (days)	Average Rate of Metal Weight Loss, mg/dm^2-day (mdd)		
		High-Purity Mg	Alloy FS-1a	Alloy PE
120	2.9	Disintegrated	74	67
135	5.0	-	450*	380
150	2.7	Disintegrated	1400*	1500

FS-1a - 3% Al, 1% Zn, 0.2 - 0.4% Mn
PE - 3.2% Al, 1.0% Zn, 0.10% Mn
* - Edge pitting noted

The water in autoclaves had a pH of about 10 at the conclusion of the tests. In the case of the alloys, the corrosion proceeds in a uniform fashion over the face of the sample. Some tendency to pit was noted on the edges of the FS-1a specimens. The high-purity magnesium disintegrates so rapidly that it has not yet been observed in the partially corroded condition.

5. Examination of Failed Zirconium Irradiation Capsules (F. L. Brown)

Cylindrical, NaK-filled zirconium irradiation capsules (fabricated of Grade III zirconium), which suddenly broke open during decanning operations following irradiation in the MTR, were examined in an effort to determine the role of irradiation in these unexpected failures. The capsules had been exposed to a thermal nvt of 2.3×10^{21}.

Normally, the capsules are readily opened by machining a circumferential groove near one end. The subject capsules, however, required extreme cutting tool pressures, whereupon transverse brittle rupture occurred in locations away from the machined groove.

Macroexamination of two of the failed capsules disclosed marked distortion of capsule walls, and bend tests of the material (compared with unirradiated material) disclosed no signal differences in ductility. Microstructures also failed to reveal any clear-cut indications of irradiation damage, and microhardness tests disclosed the irradiated material to be somewhat softer than the unirradiated comparison material. The microstructure is shown in Figure 23.

Figure 23. Photomicrograph of Failed Zirconium Capsule Material.

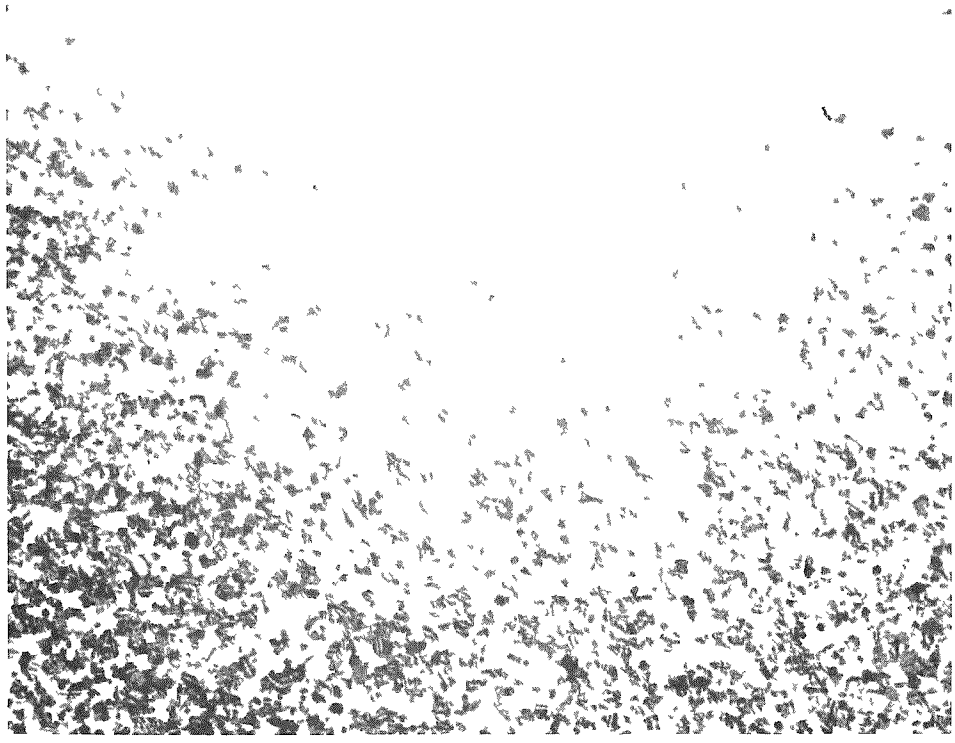

Micro 21340 Polarized Illumination 100-X

143 DPH

Based on postirradiation examination of the material, it is concluded that the apparent brittleness of the irradiated metal is at least largely due to the fact that it is Grade III zirconium, i.e., it contains impurities which make it unsuitable for reactor application.

V PRODUCTION, TREATMENT, AND PROPERTIES OF MATERIALS - ACTIVITY 5410

1. Elastic Constants of Alpha-Uranium Single Crystals (E. S. Fisher, L. T. Lloyd)

Longitudinal and shear ultrasonic wave velocities in three uranium single crystals have been obtained from measurements carried out at the Bell Telephone Laboratories in cooperation with H. J. McSkimin of the Bell Laboratories staff. The three crystals, each with 2 flat faces parallel to one of the principal crystal planes, were prepared as described in ANL-5709. The thicknesses and approximate lateral dimensions are listed in Table VI.

TABLE VI

Crystal Dimensions

Crystal	Thickness (mm)	Lateral Dimensions (Approx.) (mm)
A	2.9162	5.5 x 4.5
B	3.9185	ellipse - 5 x 4.5
C	2 7991	6 x 4.5

The apparatus for generating and detecting the high-frequency ultrasonic wave fronts is described by McSkimin and Bond.[1,2] The technique is especially designed for very small specimens. Pulsed wave trains from a 1/2" diameter quartz transducer are transmitted through a 2" long x 1/2" diameter buffer rod. This rod is tapered at the specimen end to provide a 1/8" square, finely ground, flat surface to which one of the specimen faces is sealed with a viscous fluid.

The part of the wave train which is not reflected at the specimen-seal interface propagates through the specimen in a direction normal to the sealed face and is reflected at the opposite face. Part of the reflected wave train is transmitted back through the buffer rod and is detected by the quartz crystal from which the waves originated. The resulting electrical signal is amplified, rectified and portrayed on an oscilloscope

---

[1] McSkimin, H J., "Ultrasonic Techniques Applicable to Small Solid Specimens," J. Acoustical Soc. 22 413-418 (1950).

[2] McSkimin, H. J. and Bond, W. L., "Elastic Moduli of Diamond," Phys. Rev. 105, 116-121 (1957).

screen. The wave train remaining in the specimen travels with characteristic velocity between the opposite faces. At certain frequencies, twice the specimen thickness is equal to an integral number of wave lengths; this corresponds to a resonance condition. At these frequencies the trailing reflections received at the detector will be an integral number of wave lengths apart and will give rise to a characteristic " in phase" oscilloscope pattern. The wave velocity (V) is then determined from the relation:

$$V = \frac{2t\ fn}{n}$$

where:

t = thickness of the specimen
fn = "in phase" frequency
n = integer representing number of wave lengths in

$$2t \simeq \frac{fn}{\Delta f} \ ;$$

where Δf is the average frequency difference between successive fn values.

The wave velocity is related to the elastic constants of the crystal by the equation:

$$V = \sqrt{\frac{c}{\rho}}$$

where:

c = some function of the elastic constants
ρ = density.

To determine which fundamental elastic constants are involved in the factor c as a function of specimen orientation with respect to the propagated waves, the theory of thickness vibrations in infinite plates[3] is used for small crystals of the type studied here. Because the specimens are not actually infinite plates, the measured velocity is affected by the lateral dimensions at low frequencies. For this reason it is necessary to measure the velocity over a range of frequencies. As frequency increases, the influence of the lateral dimensions becomes less and the velocity approaches a lower limiting value asymptotically. This asymptotic value is then used to calculate the elastic constants given by the theory. The wave velocities in the present specimens were measured over a range of frequencies from 50 to 180 megacycles.

---

[3] Cody, Walter, Piezoelectricity, McGraw-Hill Book Co., Inc., New York, p. 55 (1946).

In this technique the precision of the measurements depends primarily on the resolution of the oscilloscope pattern into successive peaks. Weak or distorted signals will increase the uncertainty in delineation of the "in phase" pattern. These adverse conditions result from absorption or scattering of pulse energy within the specimen or at the reflecting faces. The twin boundaries, which were known to be present in all three specimens, were expected to be a major source of scattering. Because these boundaries were primarily parallel to $\{130\}$ planes the effect was expected to be most important in crystals A and B; in crystal C the $\{130\}$ boundaries are parallel to the propagation direction. In line with expectations very little difficulty was experienced in determining the "in phase" frequencies for both longitudinal and shear waves in crystal C. Reflections could be detected for frequencies up to 180 Mc, although the signals became weaker at the higher range. In crystals A and B fewer distinct reflections were resolved in an individual wave train, making detection of the "in phase" condition more tedious; for these crystals no measurements were made at frequencies above 80 Mc.

The velocities calculated from the "in phase" frequency data for all three specimens indicate that the uncertainties in the measurements were relatively small. Maximum deviations from the least mean square fitted curves of velocity as a function of frequency were approximately 0.01% for all modes of vibration. The velocity derived from the 60-Mc frequency measurements for all modes of vibration was approximately 0.03% higher than the corresponding minimum limiting velocity. These limiting velocities are listed in Table VII. Elastic constants C_{ii} are calculated directly from the data and independently of each other. The theoretical X-ray density of 19.04 g/cm^3 (reported by Mueller) was used for the calculations.

TABLE VII

Elastic Constants Of Alpha-Uranium Single Crystals In The Three Principal Directions At 25° ± 0.02°C

Crystal	Mode of Vibration	Direction of Propagation	Direction of Particle Motion	Velocity (cm/sec)	Elastic Constants ($C_{ii} = \rho V^2 \frac{\text{dynes}}{\text{cm}^2} \times 10^{-12}$) ($\rho$ = 19.04 g/cm^3)
A	longitudinal	[100]	[100]	335,835	C_{11} = 2.14743
	shear	[100]	[010]	197,585	C_{66} = 0.74332
	shear	[100]	[001]	196,388	C_{55} = 0.73434
B	longitudinal	[010]	[010]	322,942	C_{22} = 1.9857
	shear	[010]	[100]	197,587	C_{66} = 0.74333
	shear	[010]	[001]	255,514	C_{44} = 1.24307
C	longitudinal	[001]	[001]	374,548	C_{33} = 2.67105
	shear	[001]	[100]	196,350	C_{55} = 0.73405
	shear	[001]	[010]	255,792	C_{44} = 1.24779

The accuracy of the data is indicated by the agreement between equivalent shear modes in different specimens. For example, in crystal A the shear mode vibrating in the [010] direction should have the same velocity as the shear mode in crystal B vibrating in the [100] direction, since they both involve only the constant C_{66}; however, due to differences in specimen shapes and errors in aligning the crystal axes normal to the propagation direction one might expect differences in these velocities even with the most precise data. The differences encountered are, however, very small compared to the deviations of other experimental determinations of elastic constants reported in the literature. The 2 values of C_{44} differ by 0.4%, the C_{55} difference is 0.04% and for C_{66} the difference is 0.001%.

Three crystals which are to be used for deriving the cross constants C_{12}, C_{13} and C_{23} (ANL-5709) are now being prepared. Each crystal will have 2 faces perpendicular to one of the principal planes, but the normals to these faces (the propagation direction) will be at some angle to the 2 principal directions in that plane.

2. Recrystallization of Heavily Cold Rolled Uranium Sheet (W. R. Yario, L. T. Lloyd)

The data reported in ANL-5643 and ANL-5709 on the recrystallization of heavily cold rolled uranium sheet showed distinct changes in mean expansion coefficient for specimens annealed for 15 hours at temperatures between 320° and 400°C. The change in coefficient was not a simple function of the measured volume per cent recrystallization. At low annealing temperatures and correspondingly low percentages of recrystallization the coefficient changed very little, whereas at higher temperatures and greater percentages of recrystallization the change in coefficient was more pronounced. An additional specimen has now been annealed at 370°C for 15 hours and, although it was 58% recrystallized, the expansion coefficient changed only slightly from the as-rolled value. These results suggest the possibility of a different recrystallization mechanism operating at annealing temperatures below 380°C than that above that temperature.

Specimens annealed for varying periods of time at 360° and 400°C were studied metallographically. The annealing times along with the corresponding volume percentages of recrystallization are given in Table VIII. The extreme heterogeneity of deformed and annealed microstructures in this material has been noted previously (ANL-5623), and further observations will not be discussed in detail here. The comments will be limited to a particular type of structure representing the larger portion of the recrystallized material for each specimen.

As shown in Figure 24, there appear to be two recrystallization processes operating. The relatively large grains in the process of absorbing extremely fine recrystallized grains appeared to varying degrees in all

TABLE VIII

Volume Per Cent Recrystallization of Heavily Cold Rolled Uranium Sheet After Annealing

Annealing Treatment		Volume Per Cent Recrystallization
Time	Temp, °C	
15 hours	360	29, 26,* 30*
92 hours	360	74
165 hours	360	81
5 minutes	400	36
15 minutes	400	55
30 minutes	400	67
1 hour	400	77
15 hours	400	97,* 96,* 94,* 98*
92 hours	400	100

* Values determined after testing dilatation samples.

the specimens except those annealed at 400°C for periods of 15 hours or more. Figure 24-a is an early stage of the process, where there is some unrecrystallized material separating the bands of fine recrystallized grains. After 92 hours at 360° C some larger grains have appeared (Figure 24-b), and after 165 hours the process has neared completion, as shown in Figure 24-c. The specimen annealed for 15 minutes at 400°C (Figure 25) showed the same type of areas as did the specimens annealed for 5 and 30 minutes at 400° C. There is some evidence for preferential growth of the larger grains in Figure 25, because they have similar tones of gray when observed in polarized light.

The fine recrystallized grains are believed to occur in areas that were the most heavily deformed during rolling, for they are the first areas to appear as recrystallized metal in samples of low per cent recrystallization. Subsequent to their formation, the larger grains grow within these areas. These processes appear to occur simultaneously at both temperatures; however, the large grain growth lags the formation of fine grains more for the 360° C annealed samples than it does for the 400° C annealed samples.

Figure 26 is a plot of volume per cent recrystallization as a function of the logarithm of annealing time for the 360° and 400° C annealed samples. The 400° C curve could be broken into two segments with a discontinuity occurring at approximately 5 hours, and a similar phenomenon may occur for the 360° C curve. This again suggests the occurrence of two recrystallization processes.

Figure 24. Heavily Cold Rolled Uranium Sheet Annealed at 360°C for Various Periods of Time.

24-a. Annealed 15 Hours

Micro 21347 P.L. 400-X

24-b. Annealed 92 Hours

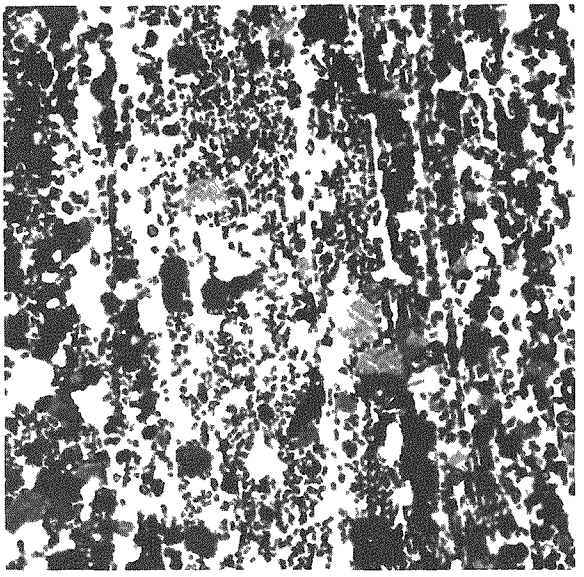

Micro 21324 P.L. 400-X

24-c. Annealed 165 Hours

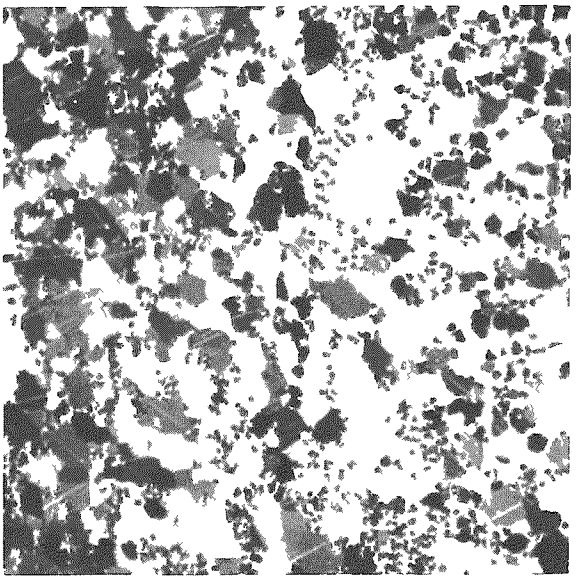

Micro 21434 P.L. 400-X

Figure 25. Heavily Cold Rolled Uranium Sheet Annealed for 15 Minutes at 400°C.

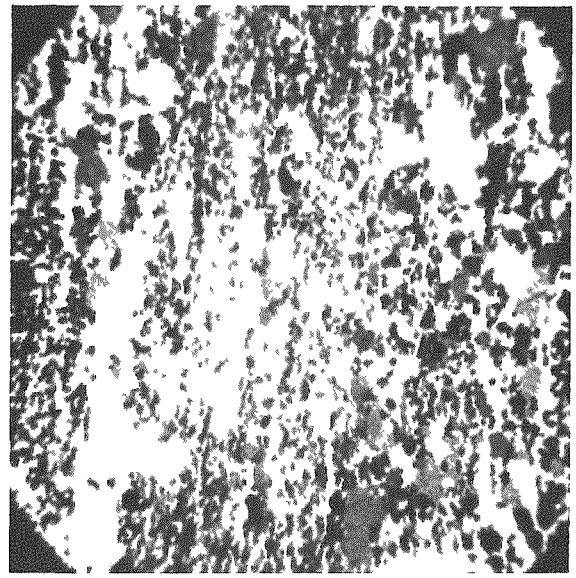

Micro 21381 P.L. 1000-X

Figure 26. Volume Percent Recrystallization of Heavily Cold Rolled Uranium Sheet as a Function of the Logarithm of Annealing Time at 360° and 400°C.

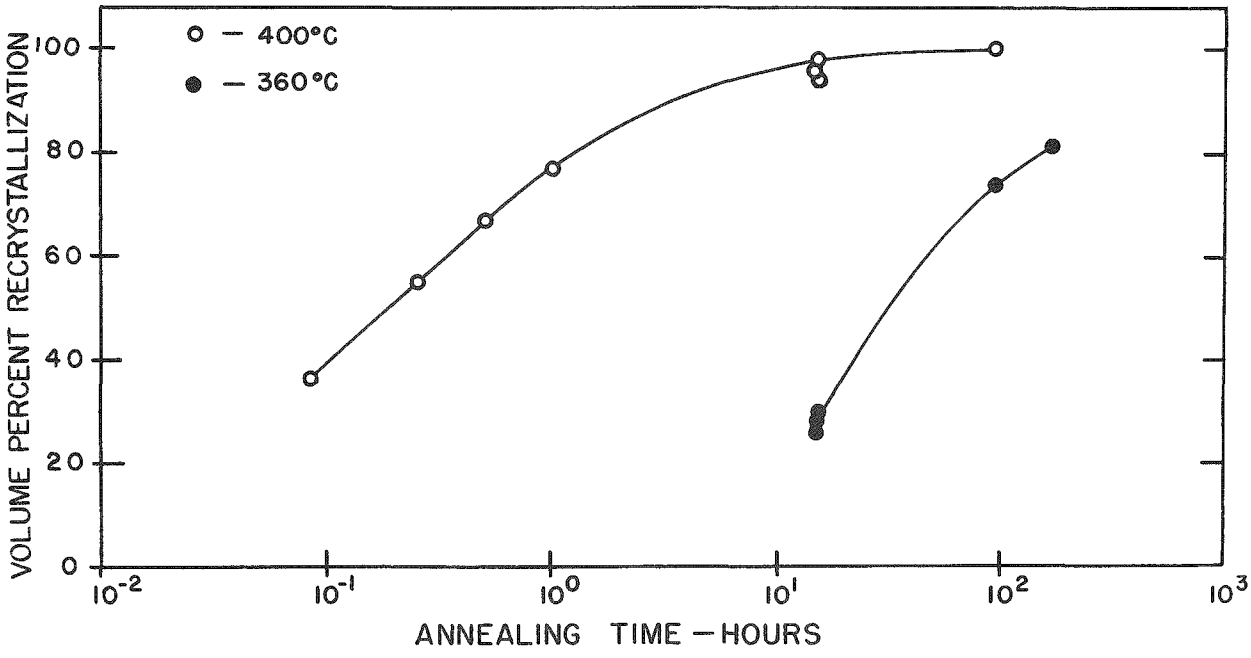

Macro 21440

If the occurrence of two recrystallization processes is accepted it is probable that the formation of the fine grains is associated with only a small change in mean expansion coefficient and, therefore, with little or no texture change, whereas the growth of the larger grains is related to a greater change in mean expansion coefficient and a greater texture change. This problem can be clarified by studying the mean expansion coefficients of samples annealed for long periods of time at low annealing temperatures and samples annealed for short periods of time at high annealing temperatures. These experiments are being performed.

3. Self-Diffusion in Uranium (S. J. Rothman, L. T. Lloyd)

Attempts to measure the self-diffusion coefficients of polycrystalline uranium in the alpha or gamma phases have so far been unsuccessful. The experimental difficulties that have been encountered are discussed below. As the alpha-phase diffusion coefficient is expected to be several orders of magnitude smaller, and therefore more difficult to measure than that near the top of the gamma phase, work on diffusion in the alpha phase has been temporarily discontinued until results are obtained in the gamma phase.

The long-time diffusion experiment mentioned in ANL-5709 has been terminated. The quartz capsule had slagged onto the nickel block and broke when the specimen was being removed from the furnace. Further attempts to produce a sample for diffusion by sputtering have resulted in oxidation of the sample surface.*

Oxidation of either the sample or the sputtered metal could easily cause the "barrier layer" mentioned in ANL-5709. Therefore every attempt has been made to eliminate this contamination. The entire sputtering system has been leak hunted, the pumps have been cleaned, and the last two elements on the gas train have been changed. Notwithstanding this, the sputtered layers still oxidized during deposition.

Variations were then made in the sputtering routine. It was observed that if the U^{235} cathode was cleaned by ionic bombardment for about 5 - 10 minutes, it became discolored. It is not known whether the cathode itself oxidizes, or whether material that has been sputtered off oxidizes and diffuses back to the cathode. Further bombardment, for about a half-hour, cleans the cathode. As the cathode had been cleaned for much shorter times in previous runs, a barrier layer may well have been deposited onto the specimen.

---

* Oxidation as used here includes surface reaction with nitrogen or any other gas.

One sputtering experiment has been carried out in which the cathode was given a thorough preliminary cleaning. To avoid surface roughening of the specimen (see below), the sputtering current was cycled up and down during U^{235} deposition. The sample discolored when the current was lowered, but cleaned when the current was raised high enough. Presumably, gases are released from the cathode and other objects which are heated or bombarded. Further experiments are being run to see if oxidation can be avoided.

Surface roughening of the sample was mentioned briefly in ANL-5709. Recently it was observed that this deformation takes place during deposition by sputtering. An experiment with a thermocouple inside the specimen has shown that its temperature may rise to 450° C when the specimen is grounded (the positive terminal of the power source is also grounded). However, if the specimen is allowed to float, i.e., it is not grounded, its temperature does not rise above about 270° C for the same current, and the surface is not roughened badly. This is undoubtedly due to the elimination of the electron bombardment that every grounded object in the bell jar must undergo.

It seems reasonable that the specimen should be subjected to the same intensive cleaning as the cathode. This has not been done in the past and may also be a cause of the "barrier layer." It is questionable whether the specimen can be bombarded for half an hour without roughening or etching.

4. The Uranium-Carbon System (B. Blumenthal)

Work on this program during the past quarter has been concerned with the determination of the transformation temperatures of U-C alloys. Because the U-UC solid-to-liquid transformation temperature is believed to be very near the melting point of pure uranium, it was necessary to redetermine the latter with the same equipment to establish a reliable reference point. Past works of Dahl and Cleaves[4] and Blumenthal[5] have shown the alloy composition to change with consecutive thermal analyses. To overcome this difficulty it was necessary to make repeated measurements, i.e., cycle the metal around the melting point range.

Apparatus: The apparatus, built to permit repeated thermal analyses at predetermined variable rates, consists of a Globar resistance vacuum furnace controlled by a Minneapolis-Honeywell pneumatic controller. The program control is imposed by a cam cut to suit the desired cycling pattern. The furnace has a low heat capacity so that it follows the

---

[4] Dahl and Cleaves, J. Research, Natl. Bur. Stds. 43, 513-517 (1949).

[5] Blumenthal, B., ANL-5349.

predetermined cycle with little lag. It is heated by two separate sets of Globars, one providing the manually adjusted base load (about 2/3 of the total) and the other the control load. The 6" vacuum system has been described previously.[6]

The urania crucible with the metal and the thermocouple in its center is suspended in the furnace and the thermocouple is protected by a urania tube. Suitable precautions are taken to shield the crucible with the melt from the cold sections of the furnace tube and establish a uniform temperature gradient around the melt. In spite of the sensitivity of the uranium refractories to thermal and mechanical stresses the arrangement proved to be highly successful provided the system was not cooled to room temperature during an experimental run. Up to eight cycles have been made without failure in a range of ± 40°C around the melting point in a period of 32 hours. A pressure of 5 to 7 · 10^{-7} mm Hg was maintained throughout each series of cycling experiments.

The temperature is recorded by a specially built Leeds - Northrup Speedomax recorder with a span of 3 millivolts and ranges beginning at 0, 2.5, 5, 7.5 and 10 mv. Its sensitivity is ± 0.003 mv and its error is within ± 0.009 mv when calibrated against a Rubicon precision potentiometer. The Pt-10% Rh/Pt measuring thermocouple was calibrated against a standard thermocouple which had been calibrated by National Bureau of Standards and reported to have an uncertainty of 0.3°C at 1100°C. Calibrations were made before and after each run or group of runs. The precision of these calibrations was ± 0.003 mv. Repeated measurements of the same transformation on either heating or cooling were made with a precision ranging from 0.002 to 0.007 mv (standard deviation)

The Melting Point of Uranium Dahl and Cleaves[4] have determined the solidification temperature of uranium, apparently on a relatively pure biscuit metal of low carbon content, and found it to be 1132° ± 1°C. They used an optical method and melted in an inert atmosphere in a variety of crucible materials. Baumrucker and Chiswik[7] determined the transformation temperatures on high-purity uranium using urania crucibles in vacuo. Their data, however, were too low, due to an error in the thermocouple calibration,[8] the corrected data[9] are given in Table IX.

---

[6] Blumenthal, B., ANL-5019.

[7] J. E. Baumrucker and H. H. Chiswik, ANL-5036; also BMI-1000.

[8] J. E. Baumrucker, Personal Communication.

[9] B. Blumenthal, Personal Communication.

TABLE IX

Melting Point of Uranium

Investigator	Transformation Temperature, °C		
	$\gamma \longrightarrow$ liquid	liquid $\longrightarrow \gamma$	Mean of Melting and Freezing
Dahl and Cleaves		1132 ± 1	
Baumrucker and Chiswik	1131.8 ± 0.5	1132.1 ± 0.5	
Present Work (Blumenthal)	1131.8 ± 0.4	1133.0 ± 0.4	1132.4 ± 0.6

Two ingots of high purity uranium were studied; the rates of both heating and cooling were 0.74°C/minute. Good arrests of about 22-minute duration were obtained during the seven cycles made on each ingot. The corrected mean transformation temperature data are given in Table IX. They are in excellent agreement with those by Dahl and Cleaves and the corrected data by Baumrucker and Chiswik. It is worth noting that no supercooling phenomena were observed and that the freezing point data are slightly higher than those for the melting point. The reason for the latter is not known; however, it may be explained by the presence of a temperature gradient between the melt and the thermocouple which is shielded by a rather poorly conducting refractory. This temperature gradient persists throughout the long arrests and causes the measured temperature to be lower during heating and higher during cooling. Assuming that the gradients are the same on heating and cooling, it is permissible to take the mean value of the melting and freezing temperatures for the true solid-liquid transformation point.

The Eutectic Temperature of the U-UC Alloys: One series of 6 cycles has been made so far. The material was high-purity uranium, induction-melted at 1400°C in a high-purity graphite crucible, and cast in a water-cooled copper mold. No carbon analytical data were obtained to date, but the material was prepared to contain at least several hundred ppm of carbon. The first two cycles gave very satisfactory arrest temperatures of about 22-minute duration, both on melting and freezing, at a rate of 0.74°C/minute. On subsequent cycles, however, the curves began to assume a slope and the arrest temperature became less distinct, although the midpoint of each sloping arrest could still be measured. This is due to the composition changes during the experiment. The data are listed in Table X. The one set of data obtained to date shows that the U-C system is a eutectic system with a eutectic temperature at 1116.6°C. This transformation point falls considerably lower from the melting point of pure uranium

TABLE X

Eutectic Temperature Measurements Of Uranium-Carbon Alloy

Ingot Number	Cycle Number	EMF in Millivolts (Pt-10% Rh/Pt Thermocouple)	
		Melting	Freezing
B723	I	10.896	10.899
	II	10.894	10.897
	III	10.880	10.888
	IV	10.874	10.912
	V	10.896	10.897
	VI	10.883	10.900
Mean of I and II		10.895	10.898
Mean of I to VI		10.887	10.899
Correction for:			
Thermocouple		-0.0056	-0.0056
Instrument		+0.0464	+0.0489
Eutectic Temp:		(in °C)	
from I and II		1116.4	1116.9
from I to VI		1116.1	1116.9
Mean of Melting and Freezing:			
I and II		1116.6 ± 0.2 °C (standard deviations)	
I to VI		1116.5 ± 1.1 °C	

than was anticipated; the data need further confirmation. It is intended to do this by cycling a high-purity melt in a graphite crucible, thereby increasing rather than decreasing the carbon concentration during thermal analysis.

Extrapolation of the previously determined liquidus curve to the eutectic temperature of 1116.6°C yields a eutectic concentration of 160 ppm by weight, or 0.32 atomic per cent.

The α - β Transformation of Uranium: The usefulness of the apparatus in the above experiments suggested its application to the solid state transformations in the uranium-carbon system. To establish a reference point, the α - β transformation of the pure metal was redetermined. The ingots were left in the crucible after melting point determinations and the system brought slowly to the desired temperature level. The cycling stresses eventually cracked the crucible during the last cycle in the solid state.

Nineteen cycles were made on high-purity ingot B724 at rates ranging from 0.5° C/minute to 2° C/minute. The data are listed in Table XI.

TABLE XI

Alpha-Beta Transformation Temperatures of
High Purity Uranium (Ingot B724)

Heating or Cooling Rate (°C/minute)	Corrected Mean Transformation Temperature (°C)	
	Heating	Cooling
2	672.3	661.3
1	671.7	662.1
0.67	671.4	663.1
0.5	671.5	663.0
0.5*	671.9	662.6

*Direct potentiometric measurement

Both supercooling and superheating occurred. The latter became evident when, after the last automatic cycle, direct potentiometric measurements were made by means of a Rubicon potentiometer and a galvanometer. The spread between heating and cooling decreased from 11.0° to 8.5° C as the rate decreased from 2 to 0.5° per minute. A plot (Figure 27) of the transformation temperatures versus the logarithm of the rate indicates that the present data form a satisfactory continuation of Duwez[10] data for high-purity uranium obtained at much higher rates of cooling. The left end of the curve may reasonably be considered to be a straight line. Application of the method of least squares to the heating and cooling rates of present data yields the functions:

$$T_H = 671.8 + 0.064 \log r$$

$$T_C = 662.2 - 0.151 \log r \quad ,$$

where T_H and T_C are the transformation temperatures in °C on heating and cooling, respectively, and r the rate of heating or cooling in °C/minute. The two lines intersect at 669.0° C which may be regarded as the equilibrium temperature of the alpha-beta transformation of high purity uranium. Similar experiments on U-C alloys will be made.

---

[10] P. Duwez, J. Applied Physics 24, 152-156 (1953).

Figure 27. Effect of Heating and Cooling Rates on α - β Transformation of High-Purity Uranium.

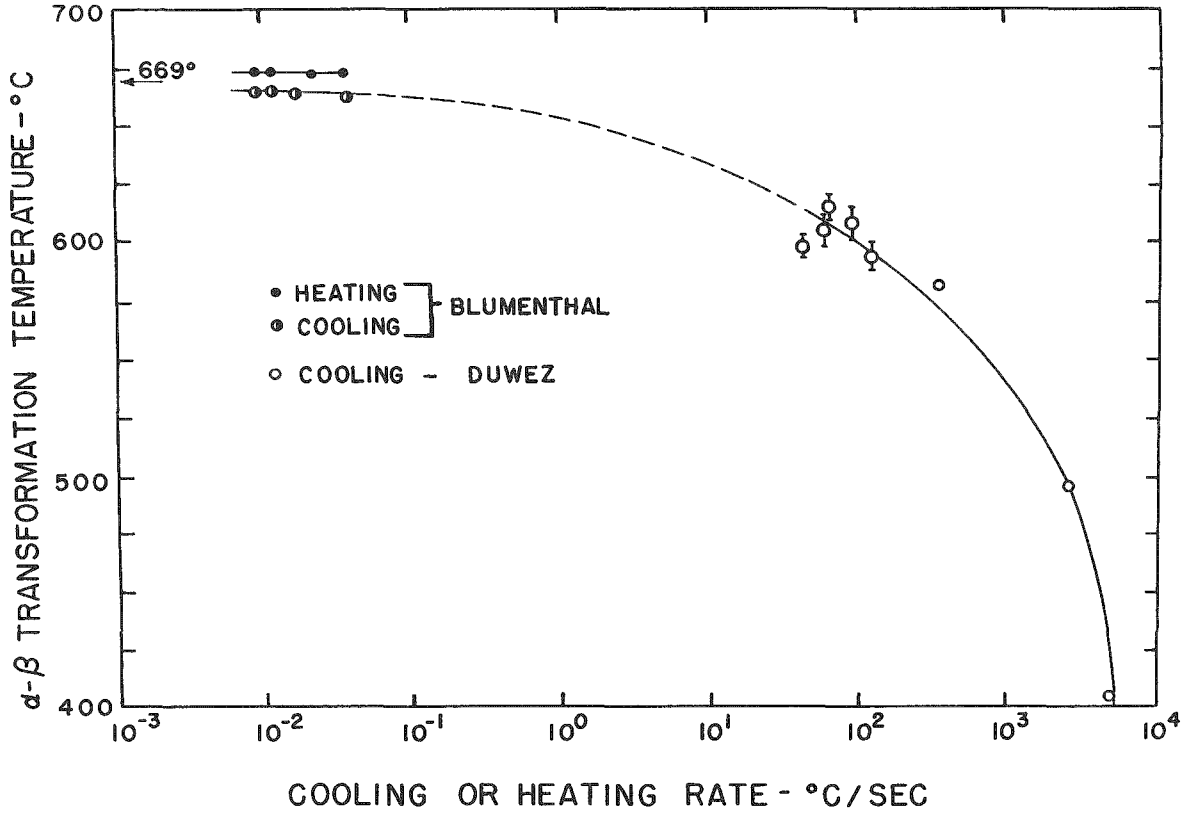

Macro 21439

5. Phase Diagrams of Uranium-Fissium Alloys (A. E. Dwight)

Uranium-Ruthenium System: The section of this binary diagram from 20 to 50 w/o Ru was investigated and the results are shown in Figure 28. Six intermetallic compounds have been found whose compositions appear to coincide with the formulas U_2Ru, URu, U_3Ru_4, U_2Ru_3, U_3Ru_5 and URu_3. Diffraction patterns have been obtained for U_2Ru, URu and U_3Ru_4. The structure of URu_3 has been reported as the L12 type by other investigators.[11] The eutectoidal decomposition of U_3Ru_5 is quite sluggish.

Uranium-Molybdenum System: The lattice parameter of the γ phase as a function of molybdenum content is being investigated. Small specimens (<1/16" thick) of six alloys made from high-purity uranium were quenched

[11] T. J. Heal and G. I. Williams, Acta Cryst. 8, 494 (1955).

Figure 28. Uranium-Ruthenium Constitution Diagram from 20 to 50 w/o Ruthenium.

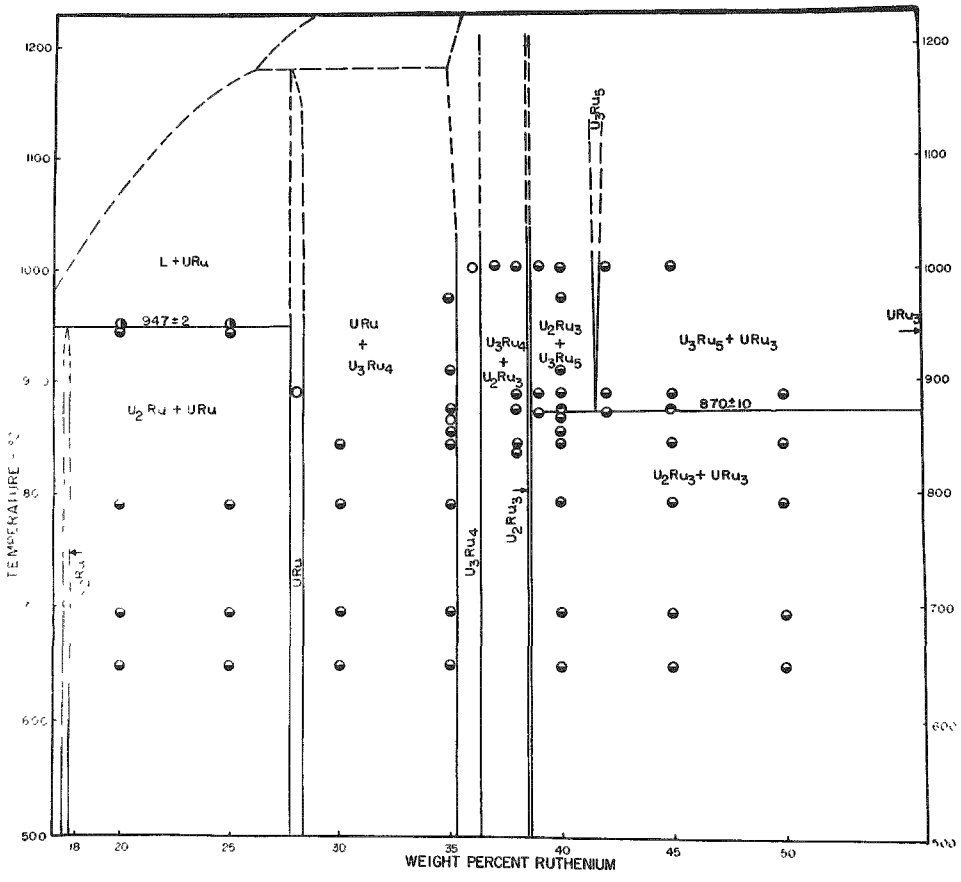

Macro 21445

from the γ range. Lattice parameters were obtained with a back-reflection camera. Data are shown in Figure 29. Data from earlier investigations are also shown for comparison. The data obtained in this current work extrapolate to 3.495 Å for pure γ uranium, a value higher than the 3.476 Å obtained by extrapolation of the earlier data. A metallographic study of the uranium-molybdenum diagram up to 10 w/o Mo has been started.

Uranium-Ruthenium-Molybdenum System: Metallographic examination of eleven ternary alloys has produced the tentative version of the uranium-rich corner of the 660° C isothermal section shown in Figure 30. The eutectoid valley originating at U-2 w/o Ru and 710° C descends quite steeply with small molybdenum additions.

Figure 29. Lattice Parameters of the γ Phase in the Uranium-Molybdenum System.

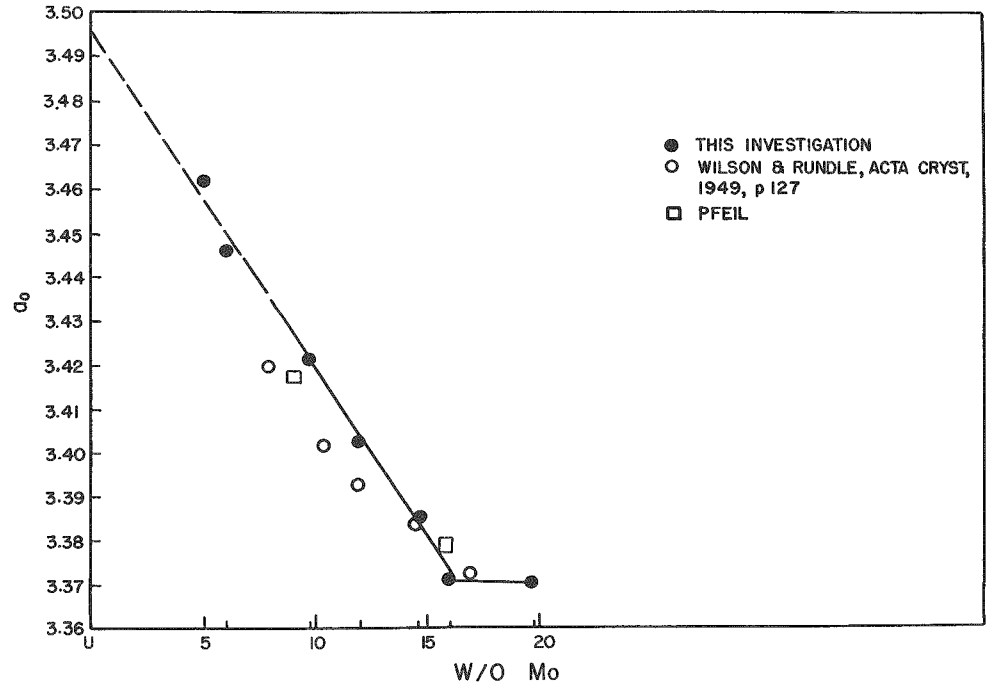

Macro 21446

Figure 30. 660°C Isothermal Section of the Uranium-Ruthenium-Molybdenum System.

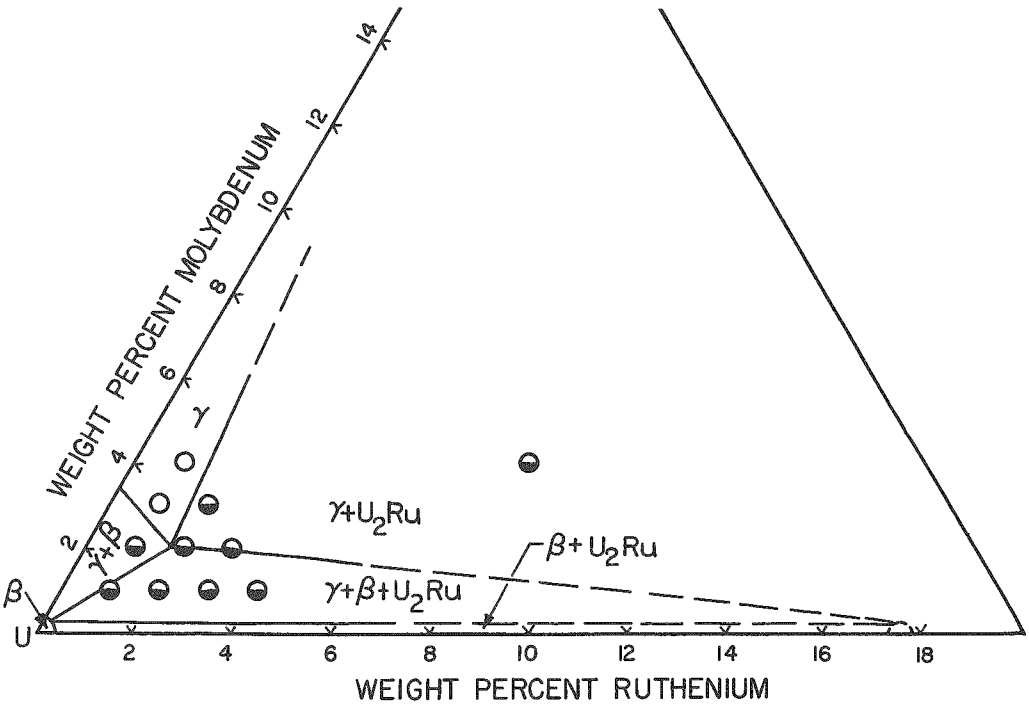

Macro 21444

6. Corrosion Mechanisms

a. Low-Temperature Aqueous Corrosion of Aluminum (S. Mori, J. E. Draley)

The long-term corrosion tests of 1100 aluminum in distilled water and in dilute potassium sulfate solutions at 50° and 70°C will be completed in the next few months; the total test duration will be nearly 1000 days. From the present data it appears that corrosion in distilled water proceeded at a continuously decreasing rate for the entire test period. Between ten days and perhaps 600 days, the gain in weight of samples is given by the following equation:

$$\Delta W = at^b \quad ,$$

where a is about 70 and b is about 0.026, when ΔW is in mg/dm^2 and t is in days. Nearly the same constants were obtained, independent of temperature (50° or 70°C) and of oxygen content (O_2 saturated or helium saturated) of the water. As far as is known, the value of the constant b is of a different order of magnitude than has ever been observed in corrosion or oxidation where this type of rate law can be applied. Beyond a certain test period weight gains became erratic, perhaps indicating that the corrosion product was no longer firmly attached.

The measured pH in water adjacent to rapidly corroding aluminum has been shown to be sensitive to the time, the distance from the aluminum surface, and the position along the sample. In all cases, the solution was alkaline close to the metal, reaching pH values from 7.8 to 9.5 before dropping as the corrosion rate diminished. This study is being made in an effort to provide explanation of the fashion in which aluminum corrodes in water and in dilute solutions.

b. Solution Potentials of Aluminum (F.E. DeBoer, J. E. Draley)

Further analysis of the reliability of the polarization curves of a number of metals in boiling distilled water has revealed that the equipment has not been giving reliable values of low polarizing currents. Improvement in this regard must be made before data can be processed.

c. Zirconium Corrosion Mechanism (R. D. Misch, F. H. Gunzel, J. E. Draley)

Improvements have been made in the techniques for measuring film resistance in vacuum at elevated temperatures. Using an electrometer, the potential which exists naturally across the oxide film as produced is measured, which, when coupled with a measurement of the current

through a known resistor, provides a means of calculating the resistance of the film. The potential rises and the film resistance drops with increasing temperature. In addition, more rapid heating of the sample to the measuring temperature is now possible.

Two ternary alloys have been screened from a number of compositions which have theoretical interest. The alloys are (1) 0.32 w/o Y, 0.68 w/o Nb, and (2) 0.03 w/o Sc, 0.47 w/o Th. Both alloys have survived 47 days in a steam test (400°C, 1500 psi steam) and have very good surface films with low weight gains similar to Zircaloy-2.

7. Mechanisms of Sintering of Ceramic Materials (L. L. Abernethy, G. C. Kucyzynski*)

Sintering studies on Al_2O_3 single spheres in vacuum, helium and electrolytic hydrogen have continued. In all cases the tungsten heaters used had been previously degassed by heating at 2200°C in a vacuum of approximately 5×10^{-7} mm Hg. The helium was purified by passing it through uranium turnings heated to 600°C, then through Linde Type 5-A Molecular Sieves, and finally through an activated charcoal trap cooled by liquid nitrogen. The hydrogen was purified by passing it through a De-oxo catalyst, followed by the Molecular Sieves and liquid nitrogen cold trap.

No sintering was observed for 15-mil spheres after heating for 3 hours at 2025°C in purified helium. (The melting point of these spheres was observed to be 2040° - 2050°C.) The spheres developed into hexagonal bipyramids during heating. Similarly, no sintering occurred in 30-mil spheres heated at 1975°C for 72 hours in vacuum (2.5×10^{-7} mm Hg). Well-developed faces were observed on the spheres as shown in Figure 31. The single crystal spheres developed 24 faces, corresponding to second-order hexagonal bipyramids, modified by an additional set of hexagonal bipyramids.

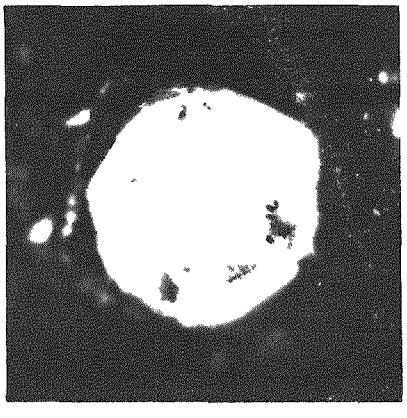

Micro 21433 50-X

Figure 31. 0.030" Al_2O_3 Sphere Fired for 72 Hours at 1975°C in a Vacuum of 2.5×10^{-7} mm of Hg.

In hydrogen, the sintering of Al_2O_3 has been observed at temperatures as low as 1800° C. Our present interpretation of this effect is that hydrogen reacts with the very pure, single crystal, alpha-corundum spheres to form oxygen vacancies at the surface, thereby promoting sintering by volume diffusion. If sintering were a result of contamination by tungsten oxide from the heater, or a reduction of Al_2O_3 by tungsten, sintering should also be observed in helium or vacuum.

The inverse slopes of log-log plots of x/r^* versus time, as determined from preliminary data, are approximately 3 for spheres heated in electrolytic hydrogen at 1825°, 4 at 1875°, and 5 at 1925° C; the mechanism of sintering of Al_2O_3 in hydrogen therefore appears to be that of volume diffusion modified by a second mechanism, i.e., evaporation condensation or surface diffusion, which is responsible for the formation of the cyrstal faces. The operation of the auxiliary mechanism would seem to depend on the temperature and on the sphere sizes. When higher temperatures or smaller spheres are used, the growth of necks between spheres proceeds rapidly and the formation of faces is less pronounced. At 1925° C, for example, the sintering of Al_2O_3 in hydrogen proceeds so rapidly that little deformation of the spheres was observed and the mechanism appears to be solely volume diffusion. Because of the formation of crystal faces at lower temperatures, only a statistical value of inverse slope can be obtained, unless the relative orientations of the spheres can be observed and the effect of crystal face development can be taken into consideration.

---

* x = length of neck formed between two spheres; r = radius of sphere.

VI. ALLOY THEORY AND THE NATURE OF SOLIDS - ACTIVITY 5420

1. Intermediate Phases in Transition Metal Systems (M. W. Nevitt)

The study of the role of atomic size in determining the occurrence and lattice parameter of Cr_3O-type phases has been completed and a paper has been submitted for open literature publication. A criterion for the stability of the phase in terms of a ratio of the radii of the component atoms has been established, and empirical equations have been derived for predicting the lattice parameter of the phases from a knowledge of the atomic radii. The parameters of these equations have been used to evaluate the suitability of certain models of the structure which can be derived from space-filling considerations. The relationship between the occurrence of the Cr_3O-type phase and the positions of the component elements in the Periodic Table has also been clarified.

Another paper has been submitted for publication giving 1200°C composition ranges and lattice parameters for three sigma phases. These data are summarized in Table XII. The existence of Os-W sigma phase has also been recently verified by Raub.[12]

TABLE XII

Approximate Composition Range and Lattice Parameters of Several Sigma Phases

System	Approximate Composition Range (a/o at 1200°C)	X-Ray Data		
		Alloy Composition (a/o)	a_o (Å)	c_o (Å)
Os-W	65 - 67 W	67 W, 33 Os	9.686	5.012
Os-Ta	65 - 75 Ta	75 Ta, 25 Os	9.934	5.189
Ir-Ta	75 - 85 Ta	75 Ta, 25 Ir	9.938	5.172

[12] E. Raub: Die Osmium-Chrom Legierungen. Ztsch. fur Metallkunde, 8, 53 (1957).